



Progressive cracking of ceramic-matrix composites
by Magadi Ravinder Joshi

A thesis submitted in partial fulfillment of the requirements for the degree of Master of Science in
Mechanical Engineering
Montana State University
© Copyright by Magadi Ravinder Joshi (1990)

Abstract:

Ceramic-matrix composites have the potential of being used in many applications particularly as high temperature structural materials for engines. Although ceramics have high strength at temperatures exceeding the melting points of the superalloys, as well as oxidation, wear and corrosion resistance, they have the drawback of low flaw tolerance. The addition of reinforcing fibers greatly improves the toughness of ceramics, but local cracking can still develop in the brittle matrix and fiber/matrix interface. Recent studies have shown that cracking of simple crossply laminates initially occurs in the transverse plies at strains considerably less than the matrix cracking strain of the longitudinal plies; longitudinal ply cracking follows. Most of the present theoretical models for cracking in crossplied composites are for polymer matrices, in which the longitudinal plies remain intact and have a constraining effect on the cracking process in the transverse plies. In ceramic-matrix composites, development of a network of transverse ply cracks is followed by longitudinal matrix cracking normal to the fibers. This cracking of the longitudinal ply causes a decrease in the ply stiffness and thus the composite stiffness. Two theoretical models are developed in the present study. These are built on the lines of the existing theoretical models for polymer matrices. The classical theory of Aveston, Cooper and Kelly is used to account for longitudinal ply matrix cracking, which is coupled with the theories of Laws and Dvorak and Nairn for transverse ply cracking. Good agreement is shown between the analytical results and the existing experimental data using the Laws and Dvorak analysis. The theory should provide a guide to the engineering use of these materials, as well as a basis for improving the materials through better understanding the parameters controlling the damage process.

PROGRESSIVE CRACKING OF CERAMIC-
MATRIX COMPOSITES

by

Magadi Ravinder Joshi

A thesis submitted in partial fulfillment
of the requirements for the degree

of

Master of Science

in

Mechanical Engineering

MONTANA STATE UNIVERSITY
Bozeman, Montana

July 1990

1378
J781

ii

APPROVAL

of a thesis submitted by

Magadi Ravinder Joshi

This thesis has been read by each member of the thesis committee and has been found to be satisfactory regarding content, English usage, format, citations, bibliographic style, and consistency, and is ready for submission to the College of Graduate Studies.

8/14/90
Date

John F. Mandell
John F. Mandell
Chairperson, Graduate Committee

Approved for the Major Department

8/14/90
Date

William E. Larsen
William Larsen
Head, Major Department

Approved for the College of Graduate Studies

8/17/90
Date

Henry L. Parsons
Henry L. Parsons
Graduate Dean

STATEMENT OF PERMISSION TO USE

In presenting this thesis in partial fulfillment of the requirements for a master's degree at Montana State University, I agree that the Library shall make it available to borrowers under rules of the Library. Brief quotations from this thesis are allowable without special permission, provided that accurate acknowledgment of the source is made.

Permission for extensive quotation from or reproduction of this thesis may be granted by my major professor, or in his/her absence, by the Dean of Libraries when, in the opinion of either, the proposed use of the material is for scholarly purposes. Any copying or use of the material in this thesis for financial gain shall not be allowed without my written permission.

Signature

M. Ravinder Joshi

Date

08/14/90

ACKNOWLEDGMENTS

I would like to acknowledge my appreciation to John F.Mandell for his patience in guiding me through my thesis work. I also would like to thank my other committee members, Jay Conant and Robert Oakberg for their perusal of my thesis report and giving important suggestions.

Special thanks goes to J.B.Schutz for his unending help in the various stages of this project. I would also like to acknowledge my appreciation to Shreeram Raj for his timely suggestions. The interaction I received from the staff and students of the Department of Mechanical Engineering, whom I have not mentioned, is deeply appreciated.

TABLE OF CONTENTS

	Page
LIST OF TABLES	vii
LIST OF FIGURES	viii
ABSTRACT	xi
1. INTRODUCTION	1
2. BACKGROUND	4
Reinforced Ceramics	4
Behavior of Ceramic Composites	5
Unidirectional Composites	5
Frictional Interaction	9
Fully Bonded Condition	11
Multidirectional Composites	12
Factors Affecting the Mechanical Behavior of CMC's	22
Interface Bond Strength	22
Temperature/Environment	24
Composite Layup	24
Residual Stresses	25
Modelling	25
Unidirectional Composites	26
Multidirectional Composites	30
Strength Approach	31
Fracture Mechanics Approach	32
Simple Fracture Mechanics Model	33
Variational Approach	34
3. THEORY	36
Predicted Behavior of CMC's Under a Tensile Load	37
Models	38
Simple Fracture Mechanics Analysis -- Self-Consistent Scheme	38
Constitutive Equations	41
Variational Approach	45
Constitutive Equations	47
4. RESULTS AND DISCUSSION	52
Applicability of the ACK Model	53
Results for the Self-Consistent Scheme	55

TABLE OF CONTENTS (Continued)

	Page
Results for the Variational Analysis	69
Comparison of the Two Theories	70
5. CONCLUSIONS AND RECOMMENDATIONS FOR FURTHER WORK	77
Conclusions	77
Comparison with the Earlier Developed Theory ...	78
Recommendations	79
REFERENCES CITED	81
APPENDICES	84
Appendix A - Parameters for the Model	85
Appendix B - Computer Flow Diagram	86
Appendix C - Computer Code for the Modified Laws and Dvorak Theory	87
Appendix D - Computer Code for the Modified Nairn's Analysis	89

LIST OF TABLES

Table	Page
1 Average Bond Strengths -- Nicalon Fiber-Reinforced Glass and Glass-Ceramics (3,16,17).....	53

LIST OF FIGURES

Figure	Page
1 A Unidirectional Lamina, the Tubular Structures Shown are the Continuous Fibers Reinforced in the Matrix Material (14).....	6
2 Types of Failure in a Typical Unidirectional CMC in the Longitudinal Direction (adapted from 14) (A) Before Failure (B) A Single Matrix Crack Propagating Through the Fibers (C) Multiple Matrix Cracks Bridged by the Unbroken Fibers	7
3 Load Transfer Between the Fibers and the Matrix (adapted from 6)	10
4 A Multidirectional Laminate with Plies Having Fibers Oriented at Different Angles (15)	14
5 Cross-ply Laminate (3)	15
6 Stress-Strain Curve for Unidirectional and Cross-plyed Nicalon/1723 Composites (4)	16
7 Longitudinal and Transverse Ply Cracking, and Delamination at the 0/90 Interface (4)	18
8 Geometry for Garret and Bailey Analysis (8)	19
9 Fracture Surface of a 0/90 Composite (4)	21
10 Interface Bond-Related Failures (3,4)	23
11 Transition from Single to Multiple Fracture as a Function of the Fiber Volume Fraction (adapted from 6)	28
12 Cracking in the Transverse and Longitudinal Plies at Increasing Strain Levels (3)	39
13 (a) Laws-Dvorak Analytical Model (b) Spacing of Two Transverse Cracks (9)	42
14 Geometry for Variational Analysis (10)	47
15 Applied Stress vs. Strain for Unidirectional Nicalon/1723. Experimental Values (o) from Ref.3	56

LIST OF FIGURES (Continued)

Figure	Page
16 Applied Stress Vs. Strain for Unidirectional Nicalon/LAS. (x) -- Theoretical Predictions; (o) -- Experimental Values (3)	57
17 Applied Stress Vs. Transverse Ply Crack Density for Nicalon/CAS Using Modified Laws and Dvorak Theory. Experimental Values (o) from Ref.3	58
18 Applied Stress Vs. Transverse Ply Crack Density for Nicalon/LAS Using Modified Laws and Dvorak Theory. Experimental Values (o) from Ref.3	59
19 Applied Stress Vs. Transverse Ply Crack Density for Nicalon/1723 Using Modified Laws and Dvorak Theory. Experimental Values (o) from Ref.3	60
20 Applied Stress Vs. Longitudinal Ply Crack Density for Nicalon/CAS Using Modified Laws and Dvorak Theory. Experimental Values (o) from Ref.3. The Ratio Shown is Between the Step Sizes of Longitudinal Ply Crack Density Parameter and That of the Transverse Ply	63
21 Applied Stress Vs. Longitudinal Ply Crack Density for Nicalon/LAS Using Modified Laws and Dvorak Theory. Experimental Values (o) from Ref.3. The Ratio Shown is Between the Step Sizes of Longitudinal Ply Crack Density Parameter and That of the Transverse Ply	64
22 Applied Stress Vs. Longitudinal Ply Crack Density for Nicalon/1723 Using Modified Laws and Dvorak Theory. Experimental Values (o) from Ref.3. The Ratio Shown is Between the Step Sizes of Longitudinal Ply Crack Density Parameter and That of the Transverse Ply	65
23 Comparison of Theoretical and Experimental Stiffness Loss for Crossplied Nicalon/CAS. Experimental Values (o) from Ref.3. Uses Modified Laws and Dvorak Theory	66
24 Comparison of Theoretical and Experimental Stiffness Loss for Crossplied Nicalon/LAS. Experimental Values (o) from Ref.3. Uses Modified Laws and Dvorak Theory	67

LIST OF FIGURES (Continued)

Figure	Page
25 Comparison of Theoretical and Experimental Stiffness Loss for Crossplied Nicalon/1723. Experimental Values (o) from Ref.3. Uses Modified Laws and Dvorak Theory	68
26 Applied Stress Vs. Longitudinal Ply Crack Density for Nicalon/CAS Using Modified Nairn's Analysis. Experimental Values (o) from Ref.3 ...	72
27 Applied Stress Vs. Longitudinal Ply Crack Density for Nicalon/1723 Using Modified Nairn's Analysis. Experimental Values (o) from Ref.3 ...	73
28 Theoretical Stiffness Loss Vs. Experimental Stiffness Loss (o) Using Modified Nairn's Analysis. Experimental Values from Ref.3, Nicalon/CAS	74
29 Theoretical Stiffness Loss Vs. Experimental Stiffness Loss (o) Using Modified Nairn's Analysis. Experimental Values from Ref.3, Nicalon/1723	75
30 (a) Applied Stress Vs. Transverse Ply Crack Density for Nicalon/LAS, Using Modified Laws-Dvorak Theory (-), Modified Nairn's Theory (*) and Experimental Values (o) (b) Similar Plot Using Earlier Developed Theory (3)	76
31 Computer Flow Diagram	86
32 Computer Code for Modified Laws-Dvorak Theory ..	87
33 Computer Code for the Modified Nairn's Theory ..	89

ABSTRACT

Ceramic-matrix composites have the potential of being used in many applications particularly as high temperature structural materials for engines. Although ceramics have high strength at temperatures exceeding the melting points of the superalloys, as well as oxidation, wear and corrosion resistance, they have the drawback of low flaw tolerance. The addition of reinforcing fibers greatly improves the toughness of ceramics, but local cracking can still develop in the brittle matrix and fiber/matrix interface. Recent studies have shown that cracking of simple crossply laminates initially occurs in the transverse plies at strains considerably less than the matrix cracking strain of the longitudinal plies; longitudinal ply cracking follows. Most of the present theoretical models for cracking in crossplied composites are for polymer matrices, in which the longitudinal plies remain intact and have a constraining effect on the cracking process in the transverse plies. In ceramic-matrix composites, development of a network of transverse ply cracks is followed by longitudinal matrix cracking normal to the fibers. This cracking of the longitudinal ply causes a decrease in the ply stiffness and thus the composite stiffness. Two theoretical models are developed in the present study. These are built on the lines of the existing theoretical models for polymer matrices. The classical theory of Aveston, Cooper and Kelly is used to account for longitudinal ply matrix cracking, which is coupled with the theories of Laws and Dvorak and Nairn for transverse ply cracking. Good agreement is shown between the analytical results and the existing experimental data using the Laws and Dvorak analysis. The theory should provide a guide to the engineering use of these materials, as well as a basis for improving the materials through better understanding the parameters controlling the damage process.

CHAPTER 1

INTRODUCTION

Ceramic-matrix composites (CMC's) are under development for structural and nonstructural applications such as heat engines, turbine blades, wear parts, and heat exchangers, at use temperatures far beyond the capabilities of metals. If CMC's maintain toughness -- resistance to rapid crack propagation -- and are able to resist attack by aggressive environments, then the low densities and low coefficients of thermal expansion of these materials make them attractive for many heat engines and hot aerospace applications. These materials have the potential of improving efficiency since they may allow operation of engineering components at higher temperatures, with lower friction, weight and inertia, as well as high thrust-to-weight ratios.

Monolithic ceramics, though they have high temperature capability and strength, are extremely brittle. A flaw as small as 10 micrometers can reduce strength to a few percent of the theoretical strength (1). This problem of brittleness can be overcome by using either (2): (i) whisker-and-particulate reinforced ceramic-matrix composites or (ii) continuous fiber-reinforced ceramics. Whisker-and-particulate composites can fail catastrophically with failure generally being matrix-controlled, while fiber-reinforced ceramics can be made to fail noncatastrophically if the fiber-matrix bonding is optimized, so that the failure is mostly controlled

by the fibers, much like current fiberglass materials.

The present work is focussed on understanding the cracking behavior of continuous fiber-reinforced ceramics. Extensive experimental work has been done previously (3), both at ambient and high temperatures, to understand the behavior of these materials. The work in Ref.3 is quite important to the present study as explained further in the ensuing chapters. A theoretical model is developed to predict the cracking behavior of CMC's. The different CMC matrix materials that were taken into consideration were: (i) lithium aluminosilicate (LAS) (ii) calcium aluminosilicate (CAS) and (iii) Corning code 1723 glass (an aluminosilicate glass). The fiber reinforcement was Nicalon (crystalline, primarily silicon carbide fibers, marketed by Nippon Carbon Company). Nicalon/1723 and Nicalon/CAS have moderate bond strength and high matrix thermal expansion coefficients, while Nicalon/LAS is less strongly bonded and has a low matrix thermal expansion coefficient. This variation in the bond strength and expansion coefficient makes it possible to compare the effects of bond strength and residual stresses on the failure behavior.

Most of the existing theoretical models of cracking are for crossplied polymer matrix composites, in which longitudinal (0°) ply matrix cracking is not observed, due to the high failure strain of the matrix relative to the fibers. But in CMC's, longitudinal ply matrix cracking accompanies the

cracking in the transverse (90°) plies. The goal of the present work is to improve the modelling of these composites by taking into account the 0° ply cracking, and its interaction with transverse ply cracking through its effect on stiffness. The approach is to use two current models for transverse cracking, and to combine these with an earlier model for 0° ply cracking. A computer routine then simulates the influence of one array of cracks on the other as the stress on the composite is increased. The predicted cracking patterns and stiffness changes are then compared with existing experimental data for three materials.

CHAPTER 2

BACKGROUND

Reinforced Ceramics

Ceramics have received widespread attention because of their inertness and stability at high temperatures combined with their low densities, low thermal expansion and relatively low thermal conductivity (2). Theoretical strengths of ceramics over a wide range of temperature compare well with the low temperature strengths of the strongest materials in common use (1). In practice, most ceramics have flaws and low toughness which lead to low tensile strength and poor resistance to thermal and mechanical shock.

Among the ways of increasing the fracture surface energy - the energy required to create a new surface in a material - and thus decreasing the brittleness of ceramics is reinforcement with particles or, especially, fibers. The toughening mechanisms in these composites are believed to be crack deflection - as the crack approaches the fiber, it cannot pass through it, as a result of which it is deflected parallel to the reinforcement - or debonding at the fiber-matrix interface. Although whisker and particulate reinforcements provide isotropic mechanical properties, improvements in fracture toughness in these composites is not as great as in continuous fiber reinforced composites. Fiber reinforced composites are therefore of considerable

importance. The fibers can increase the macroscopic flaw tolerance in the fiber direction, as well as strength, stiffness and thermal shock resistance (4). Fiber reinforced composites can provide high dimensional stability over a broad temperature range, resistance to attack by atomic oxygen, and damage tolerance (2).

Behavior of Ceramic Composites

The ceramic matrices are very brittle, having failure strains far less than the fiber failure strains. Hence, initial damage in a CMC is controlled by the matrix. Depending on the orientation of the fibers in the matrix, these composites can be classified into (i) unidirectional, in which all the fibers are oriented in the same direction and (ii) multidirectional, in which the fibers are oriented in different directions in the different layers. The behavior of these two types of composites is explained in this section.

Unidirectional Composites

In Unidirectional Composites, all of the fibers are aligned in the same direction. A representative unidirectional lamina is shown in Fig.1. In this kind of composite, usually fibers having high tensile strength are incorporated into the matrix. As a result of this, a unidirectional lamina has excellent properties in the direction of the reinforcement, since most of the applied load is carried by the fibers. However, the laminate has poor properties in the other

directions. The modes of longitudinal tensile failure that can be observed in CMC's are shown in Fig.2. If a tensile load is

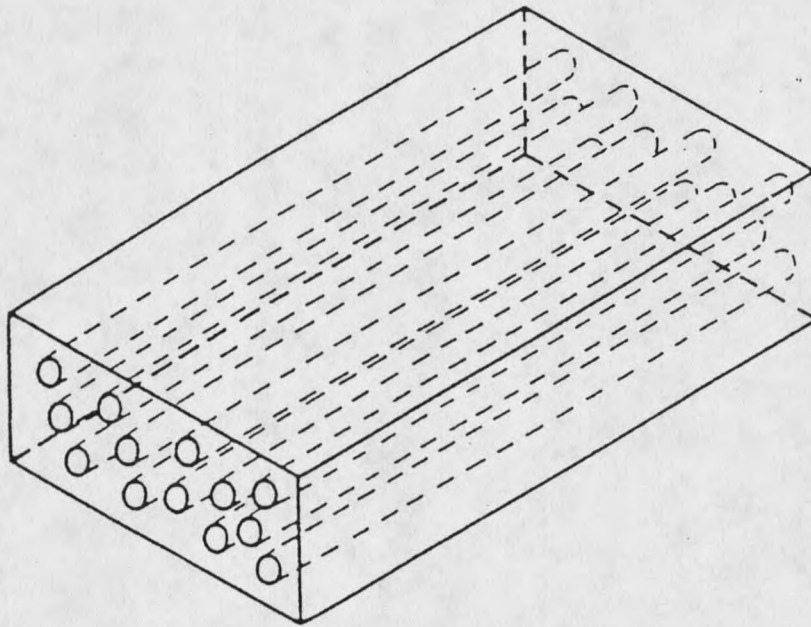


Fig.1 A Unidirectional Lamina, the Tubular Structures
Shown are the Continuous Fibers Reinforced in the
Matrix Material (14)

applied in the direction of the reinforcing fibers, the brittle matrix cracks, and if the fiber-matrix interface strength is too high the crack may propagate right through the fibers, thus resulting in the failure of the material. In a weakly-bonded material, this may not be the case, and if the proportion of the fibers is sufficient to carry the additional load shed onto them, multiple cracking of the matrix will

result. This is explained in more detail later in this chapter. For a matrix crack to occur, two conditions must be satisfied (5):

- (i) The matrix stress has to be equal to its breaking stress and

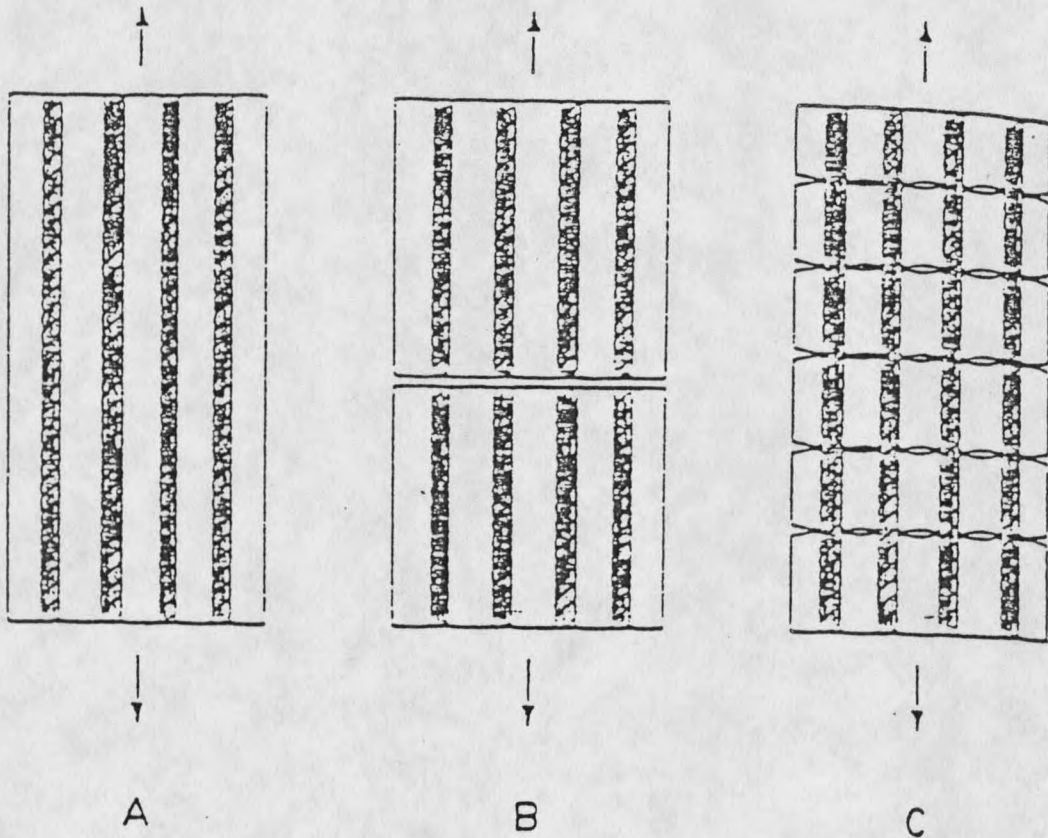


Fig.2 Types of Failure in a Typical Unidirectional CMC in the Longitudinal Direction (adapted from 14)

- (A) Before Failure
 (B) A Single Matrix Crack Propagating Through the Fibers
 (C) Multiple Matrix Cracks Bridged by the Unbroken Fibers

- (ii) There must be sufficient stored elastic strain energy to propagate the crack.

If a crack occurs in the matrix, some load is shed onto the bridging fibers. If the volume fraction of the reinforcing fibers is not sufficient to sustain the additional load thrown onto them, failure of the composite occurs at the failure strain of the matrix (4). However, if the fiber volume fraction is high, the fibers can bear the additional load, and multiple cracking occurs in the matrix. One effect of the reinforcing fibers may be to increase the failing strain of a brittle matrix by modifying the rates of release and absorption of energy during the propagation of a matrix crack (4), but this has not been well demonstrated experimentally. The critical fiber volume fraction at which a transition from single matrix fracture to stable multiple fracture occurs is given by (6)

$$V_f = \sigma_{mu} / (\sigma_{mu} + \sigma_{fu} - \sigma_f') \text{ ----- (2.1)}$$

where

σ_{mu} = breaking stress of the matrix

σ_{fu} = ultimate stress of the fibers

σ_f' = stress on the fibers when the matrix breaks

This is explained in more detail in the modelling section of this chapter. The interface (or interphase) between the fibers and the matrix is subjected to very high shear stresses, whose values depend on the difference in elastic modulus between the fibers and matrix and on the fiber volume fraction (6). At the site of the matrix crack, geometrical

stress concentrations arise, which increase the shear stresses. If the energy required to fail the interfacial bond can be supplied by the loading system or by the relaxation of stresses in the composite material, local debonding of the interface might result. Mechanical frictional forces at the interfaces help in shear stress transfer between the fibers and the matrix near the crack face, after the fibers debond. At the crack face, the reinforcing fibers carry the whole load applied to the composite, while the matrix carries zero load. The additional load thrown onto the fibers is transferred back to the matrix over a certain distance along the fiber via shear stress transfer. There are two mechanisms by which this stress transfer occurs: (i) frictional interaction, in which the interfacial stress is assumed to be constant and (ii) bonded condition, in which the fibers remain either fully or partially bonded to the matrix. These two cases have been studied by Aveston, Cooper and Kelly (ACK) (5) and Aveston and Kelly (7) respectively. The behavior of the unidirectional composites under these two kinds of interfacial stress transfer is explained briefly below.

Frictional Interaction. As explained above, the stress transfer between the fibers and the matrix is assumed to be through frictional forces in this kind of interface (see Fig.3). The fibers carry the whole load applied to the composite at the crack site, while the matrix carries no load. Over a certain distance from the crack site the additional

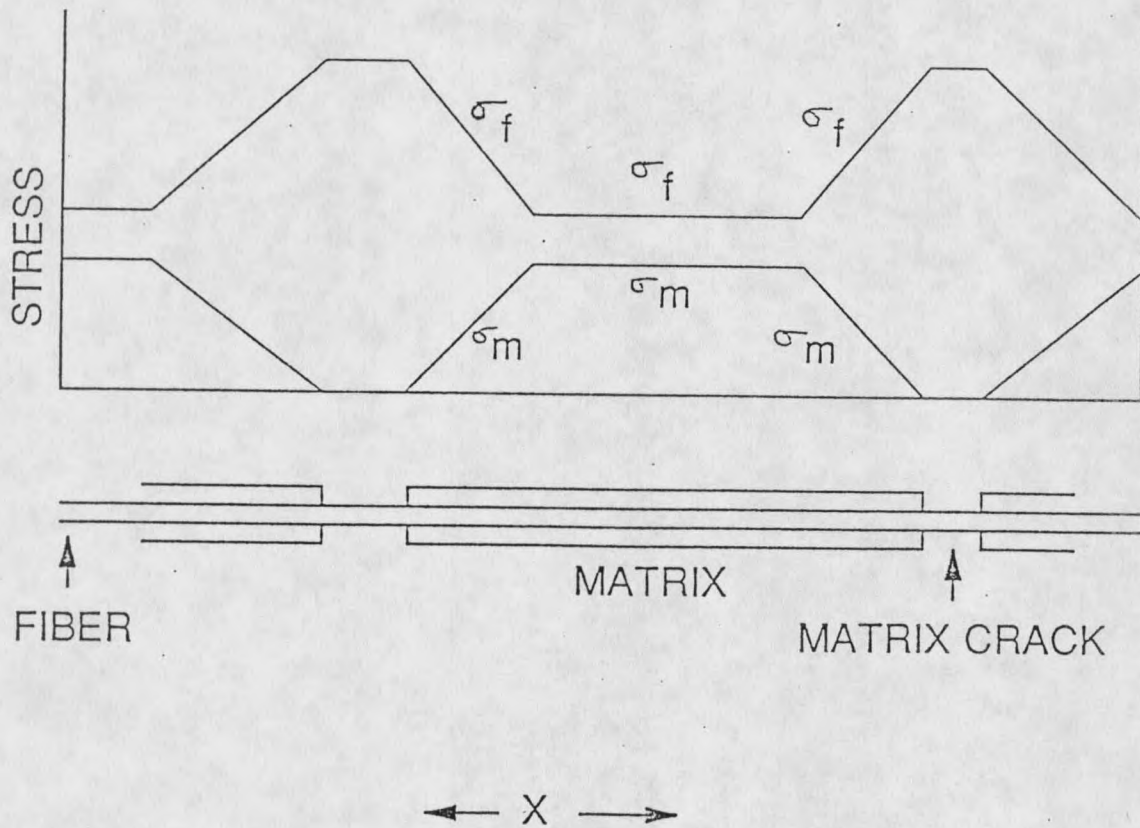


Fig.3 Load Transfer Between the Fibers and the Matrix
(adapted from 6)

load is transferred to the matrix through frictional forces until the matrix assumes its original load at some distance away from the crack. The various energy changes occurring during matrix cracking under a fixed load are given as (5):

(i) Work done by the applied stress, given as

$$\Delta W = E_c \epsilon_{mu}^2 x / \alpha \text{ ----- (2.2)}$$

(the various terms are explained in the ensuing discussion)

(ii) Work absorbed in debonding the fiber-matrix interface, Γ_{db}

(iii) The displacement of the fibers differs from that of the matrix. This implies that work done against the frictional force, τ , is equal to this force multiplied by the difference in displacement (U_s)

(iv) Reduction in strain energy in the matrix (ΔU_m)

(v) Increase in elastic strain energy of the fibers (ΔU_f)

Thus, a crack will form only if the following condition is satisfied

$$2 \Gamma_m V_m + \Gamma_{db} + U_s + \Delta U_f \leq \Delta W + \Delta U_m \quad \text{-----} \quad (2.3)$$

where Γ_m is the fracture surface work in forming a crack.

As the load is increased, the crack density - number of cracks per unit length - increases. The limiting crack spacing, after which no more matrix cracks occur, is given by

(5)

$$x' = \left(\frac{V_m}{V_f} \right) \frac{\sigma_{mu} r}{2\tau} \quad \text{-----} \quad (2.4)$$

where

V_m = volume fraction of matrix

V_f = volume fraction of fibers

σ_{mu} = ultimate strength of matrix

r = radius of fiber

τ = shear stress at fiber-matrix interface

Fully Bonded Condition. In the frictional interaction

case, the fibers and the matrix are assumed to move relative to each other, and the shear stress at the fiber-matrix interface is assumed to be constant along the fiber. In many composite systems, the fibers are well-bonded to the matrix so that the system is essentially elastic, and the interfacial shear stress is not constant, but is given by (5)

$$\tau = \frac{\tau}{2} \Delta \sigma_0 \sqrt{\phi} \exp(-\sqrt{\phi} y) \text{ ----- (2.5)}$$

where

$$\phi = \text{sqrt}(2G_m E_c / E_f E_m V_m) \ 1/(r \ \text{sqrt}(\ln(R/r)))$$

G_m = shear modulus of the matrix

$2R$ = distance between the fiber centers

y = distance from the matrix crack face

The stress distribution at a distance y from the crack face is given by

$$\Delta \sigma = \Delta \sigma_0 \exp(-\sqrt{\phi} y) \text{ ----- (2.6)}$$

where $\Delta \sigma_0$ is the stress on the fibers at the crack face.

If there is debonding near the crack site, stress transfer takes place by frictional effects over the debonded length of the fiber and by elastic effects over the rest of the length.

Multidirectional Composites

Unidirectional composites have excellent properties in the axial direction, i.e., in the direction of the reinforcing fibers. But they have poor off-axis properties. Some of the factors causing these poor properties are (4):

- (1) strain concentrations from the fibers
- (2) residual stresses
- (3) weak interfaces
- (4) porosity and other flaws

Because of these poor off-axis properties, ceramic composites are likely to find applicability mostly with multidirectional reinforcement. In this kind of composite, each ply may have different orientation of fibers. A representative multidirectional composite is shown in Fig.4. The orientation of the fibers in the various layers controls the elastic characteristics of the laminate. When a tensile stress component is perpendicular to the direction of the fiber alignment, the lamina shows poor strength and the matrix cracks at very low transverse strains, with crack propagation parallel to the fibers. The simplest form of multidirectional composites is cross-plyed composites, in which the plies have fibers oriented at an angle of 0° and 90° alternately. This kind of composite is shown in Fig.5. In the case of crossplyed laminates, the strength of an individual layer in the transverse direction is much lower than in the longitudinal direction. Hence, cracking occurs in the transverse plies (plies perpendicular to the applied tensile load) at much lower strains than in the longitudinal plies. The residual stresses complicate this by changing the stress state, and possibly causing debonding or cracking. Thus, there is often damage at very low strains, and the stress-strain curve is

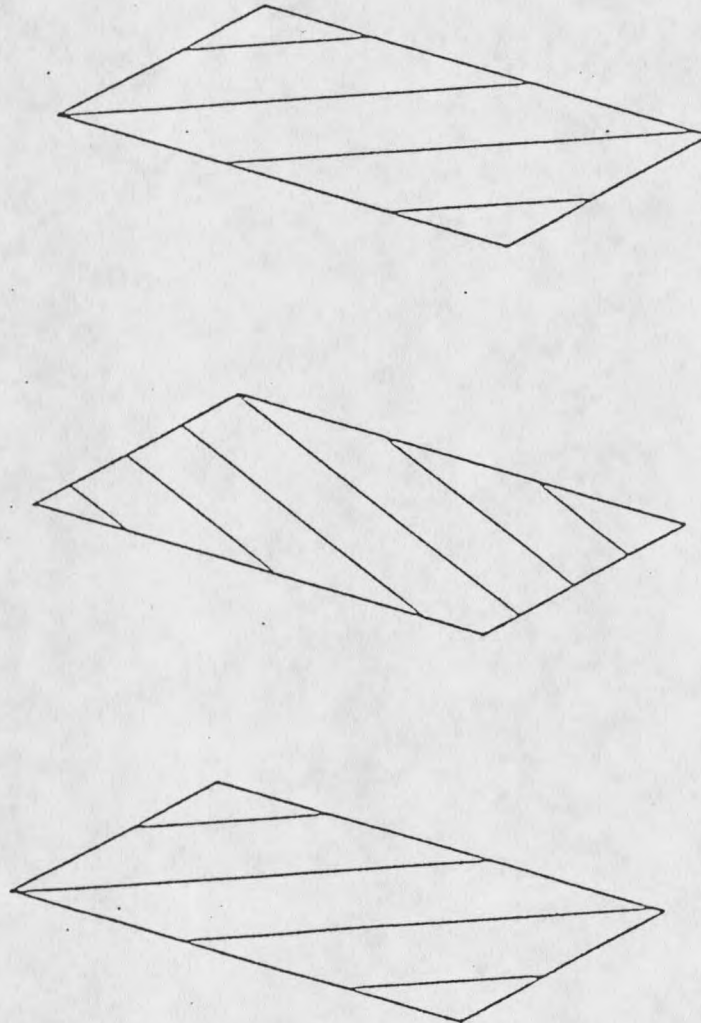
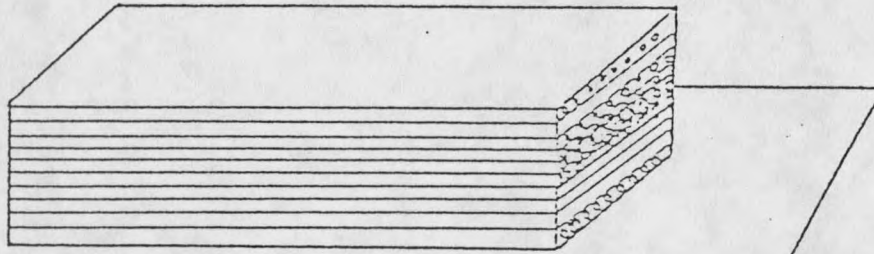


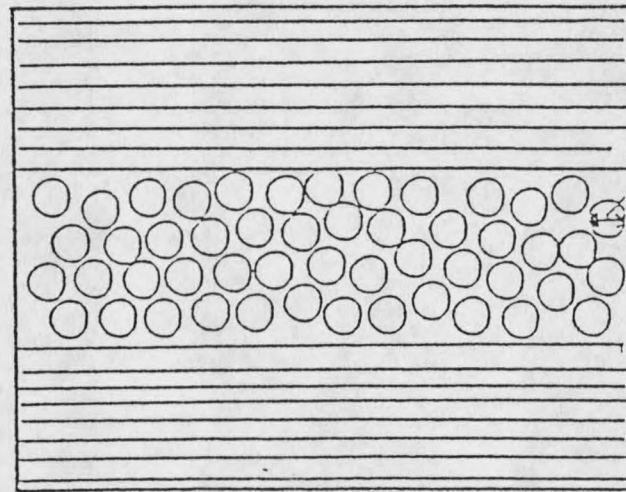
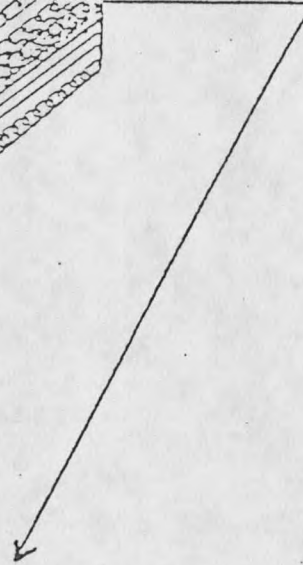
Fig.4 A Multidirectional Laminate With Plies Having
Fibers Oriented at Different Angles (15)



LAMINATE

$[0/90]_{4s}$

$V_F \cong 0.35-0.45$



FIBER DIA.
10-20 μm

0.2-0.3 mm

ENLARGED TRANSVERSE SECTION

Fig.5 Cross-ply Laminate (3)

nonlinear. This is depicted in Fig.6.

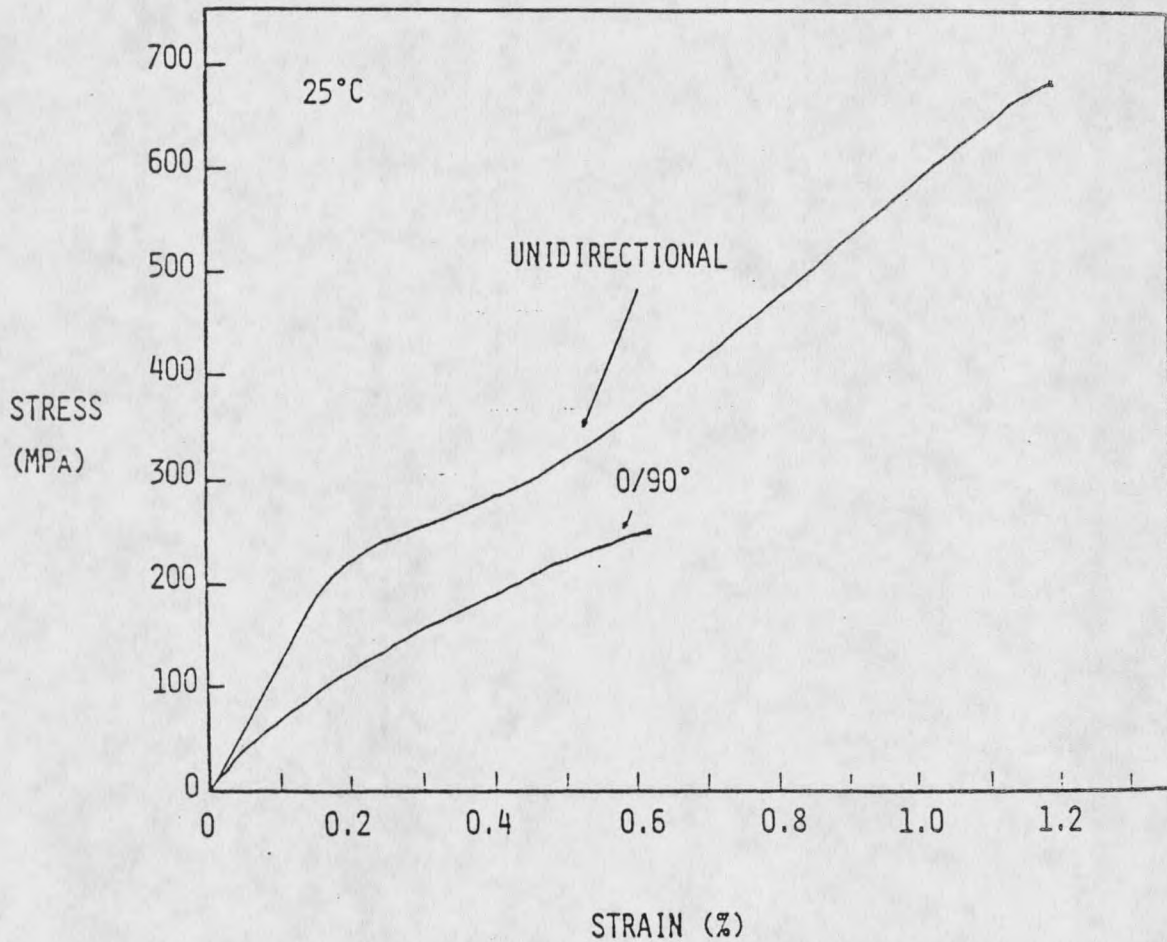


Fig.6 Stress-Strain Curve for Unidirectional and Cross-plyed Nicalon/1723 Composites (4)

Similar to the multiple matrix cracking in a unidirectional composite, multiple matrix cracking takes place in the transverse plies of a 0/90 composite under certain conditions. The stress transfer is across the interply-interface instead of the fiber-matrix interface. This shear stress may cause delamination at the interply-interface as shown in Fig.7. Although the stress transfer through the interply-interface may be through frictional interaction in rare cases, the system is usually well bonded (with the matrix continuous across the ply interface), or cracked. When bonded, the stress transfer will be elastic. The magnitude of this shear stress transfer has been analyzed by Garret and Bailey (8), based on the shear lag model. The geometry that has been used for this analysis is shown in Fig.8. The load carried by the transverse ply at the crack site is thrown onto the longitudinal plies which transfer back this additional load over a certain distance. The additional load on the longitudinal ply at a distance y from the crack site is given by the following (8) (which is similar to that given at fibers in unidirectional laminates by Aveston and Kelly (7))

$$\Delta\sigma = \Delta\sigma_0 \exp(-\sqrt{\Phi}y) \text{ ----- (2.7)}$$

where $\Delta\sigma_0$ is the stress on the fibers at the crack face.

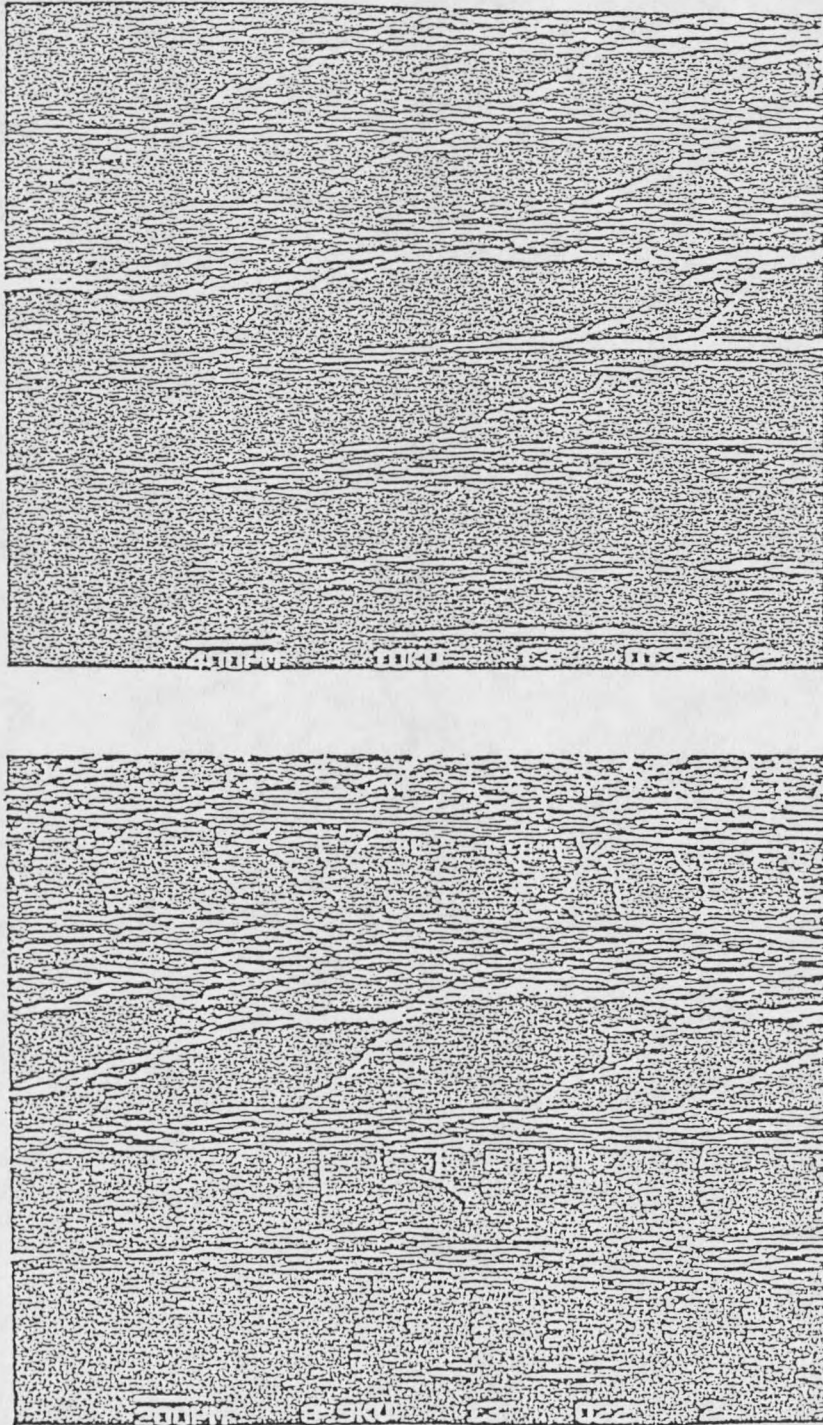


Fig.7 Longitudinal and Transverse Ply Cracking, and Delamination at the 0/90 Interface (4)

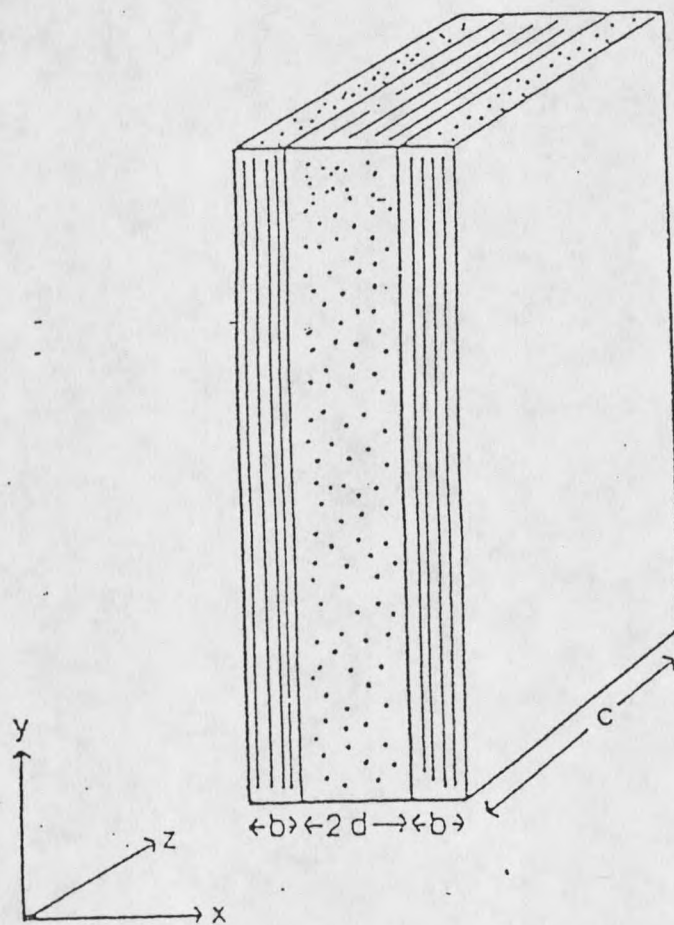


Fig.8 Geometry for Garret and Bailey Analysis (8)

$$\phi = \frac{E_c G_t (b+d)}{E_l E_t b d^2} \text{-----} (2.8)$$

where

E_c = modulus of composite.
 E_l = modulus of longitudinal ply
 E_t = modulus of transverse ply
 b, d are the thickness of longitudinal and transverse plies, respectively

They also give an expression for the shear stress transfer across the interply interface

$$\tau_i = b \Delta \sigma_o \sqrt{\phi} \exp(-\sqrt{\phi} y) \text{-----} (2.9)$$

and the load

$$F = 2bc \Delta \sigma_o [1 - \exp(-\sqrt{\phi} y)] \text{-----} (2.10)$$

where c is the width of the laminate.

With increasing strain, the crack spacing in the transverse ply approaches a limiting value, which increases with the increase in the transverse ply thickness (6). Final failure may be either debonding at the fiber-matrix interface or fiber failure (see Fig.9).

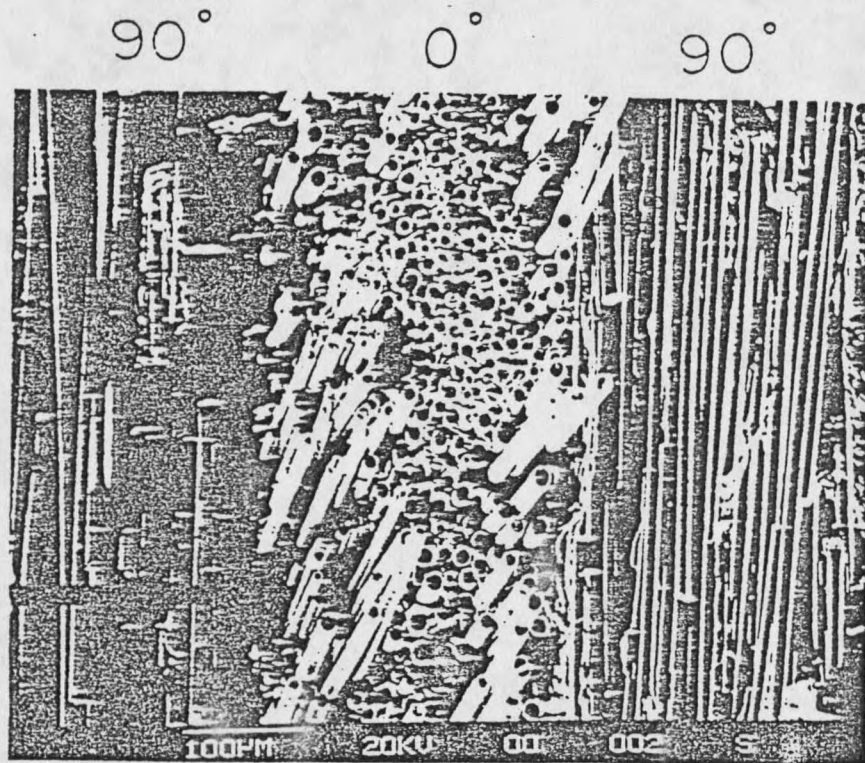


Fig.9 Fracture Surface of a 0/90 Composite (4)

Factors Affecting the Mechanical Behavior of CMC's

The toughness of a ceramic material is enhanced by the reinforcement. For a given fiber and matrix system, the various factors that affect the mechanical behavior of a CMC are (3):

- (1) Interface bond strength
- (2) Temperature/Environment
- (3) Composite layup
- (4) Residual stresses

Interface Bond Strength

In a fiber-reinforced composite, the fibers carry most of the load applied to the composite; the matrix helps in transferring this load onto the fibers, and dominates off-axis properties. This stress transfer takes place at the fiber-matrix interface. Thus, the interface plays an important role in the behavior of a fiber-reinforced composite. The quality of an interface is quantified by the interface bond strength. High bond strength is not recommended for good axial properties in CMC's, but a low bond strength will worsen the already poor off-axis properties. Also, in the case of brittle composites, a transverse matrix crack propagates right through the fibers to cause failure if the bond is too strong. This is shown in Fig.10a. When the bond is of low to moderate strength, a matrix crack is deflected parallel to the fibers (Fig.10b) or the crack propagates perpendicular to the debonded fibers (Fig.10c). The second kind of failure is

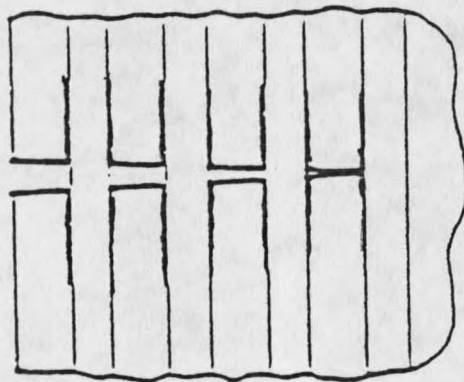
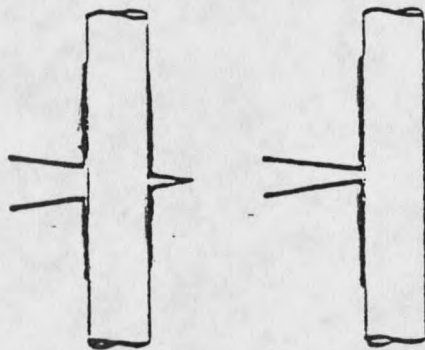
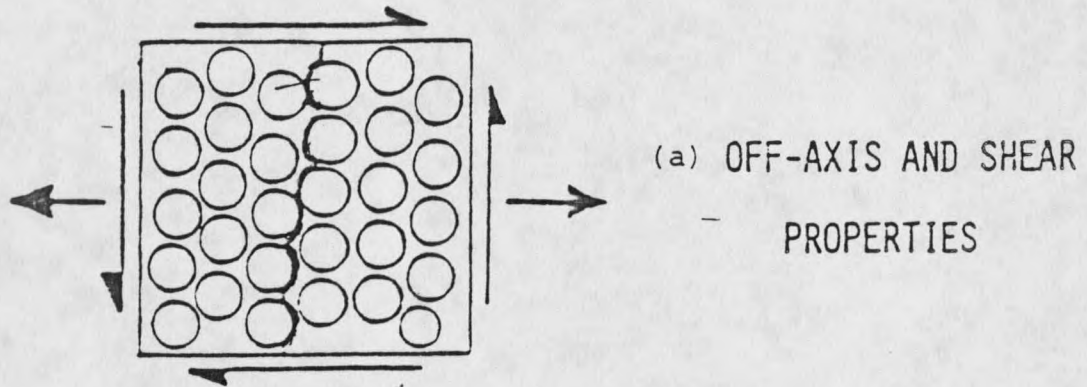
INTERFACE DOMINATED PROPERTIES

Fig.10 Interface Bond-Related Failures (3,4)

generally seen in glass and ceramic matrices (4). Thus, the interfacial bond strength has to be optimized to have good strength and toughness properties.

Temperature/Environment

This factor is crucial for CMC's, since they are intended to be used for high temperature structural applications. These CMC's should be able to withstand oxidation and other adverse conditions, caused by high-temperature exposure. Many CMC's with a carbon interphase are subject to high temperature embrittlement in the presence of oxygen (3).

Composite Layup

Fiber-reinforced ceramics show an improved performance over monolithic ceramics. They have very good properties in the direction of the reinforcing fibers, but show poor off-axis properties. Since, in practice, materials experience transverse stresses, CMC's are likely to be used in the form of multidirectional laminates. In these laminates, too, cracks occur in the off-axis plies at very low strain values. This is undesirable, particularly so for CMC's, because water and other substances enter through the crack and cause premature failure. Thus, the laminate configuration has to be designed to meet the structural requirements. This requires a thorough knowledge of the failure processes in these materials.

Residual Stresses

These are defined as the stresses that are present in a material due to cool-down from higher manufacturing/solidification temperatures to the ambient temperatures and are very important in understanding the failure processes in CMC's. They might cause matrix cracking even before the material is loaded. However, these residual stresses may sometimes be beneficial in arresting the crack growth. These stresses arise due to coefficient of thermal expansion mismatch between the fibers and the matrix, and, macroscopically, between different plies having differing fiber orientation. In multidirectional laminates, this is due to the difference in the coefficient of thermal expansion between the adjacent plies. While designing CMC's, residual stresses have to be taken into account.

Modelling

CMC's are composed of brittle constituents. The matrix and interphase control the damage development in these materials. If the fibers are strong enough to sustain the applied load, the matrix fragments into blocks too small to be loaded. Final failure occurs by delamination or fiber breakage. In the case of multidirectional laminates, damage first appears in the off-axis plies relative to the dominant tensile stress direction. The load transfer is across the interply interface instead of fiber-matrix interface as in

unidirectional laminates. Residual stresses complicate the failure processes and have to be taken into account for proper design of these laminates. This section discusses the various approaches - strength, fracture mechanics - that have been considered to model the failure of unidirectional and multidirectional laminates.

Unidirectional Composites

Understanding failure in unidirectional materials is fundamental to the study of failure mechanisms in multidirectional laminates. The classical theory of Aveston, Cooper and Kelly (5) lays the foundation to predict the cracking behavior of unidirectional composites. In their study of multiple cracking, it is reported that in a fibrous composite, if one of the constituents has a much lower breaking strain than the other, a tensile loaded specimen shows multiple fracture of the more brittle component until the specimen finally breaks at the ultimate failure strain of the stronger component. In CMC's, the fibers are much stronger than the brittle matrix. ACK theory gives the condition for the multiple fracture of the matrix as

$$\sigma_{fu} V_f > \sigma_{mu} V_m + \sigma_f' V_f \quad \text{-----(2.11)}$$

where σ_{mu} is the ultimate stress of the matrix.

This equation states that multiple fracture will occur if the ultimate failure strength of the fibers is higher than the sum of the load on the fibers when the matrix cracks plus

the additional load shed to them due to matrix cracking. These authors also give the limiting crack spacing to be between x' and $2x'$, where x' is given by

$$x' = (V_m/V_f) \sigma_{mu} r/2\tau \text{ ----- (2.12)}$$

If the volume fraction of the fibers is not sufficient to sustain the additional load thrown onto them due to matrix cracking, single crack fracture occurs as a consequence. Fig. 11 shows the critical values of fiber volume fraction for the transition from single to multiple fracture of the matrix. The stress transfer mechanism that has been considered is the simple frictional interaction at the fiber-matrix interface. The final stiffness of the composite is given by (5)

$$E_o = \frac{E_c}{\left(1 + \frac{\alpha}{2}\right) \left[2px' + \frac{1-2px'}{1 + \frac{\alpha}{2}} \right]} \text{ ----- (2.13)}$$

where

$$\alpha = (E_m V_m) / (E_f V_f)$$

p = crack density

Using a simple energy balance analysis, ACK arrived at the following expression for the matrix fracture strain, ϵ_{muc} , modified from its initial value, ϵ_{mu} , by the presence of the reinforcing fibers

$$\epsilon_{muc} = \left(\frac{12\tau\gamma_m E_f V_f^2}{E_c E_m^2 r V_m} \right)^{1/3} \text{ ----- (2.14)}$$

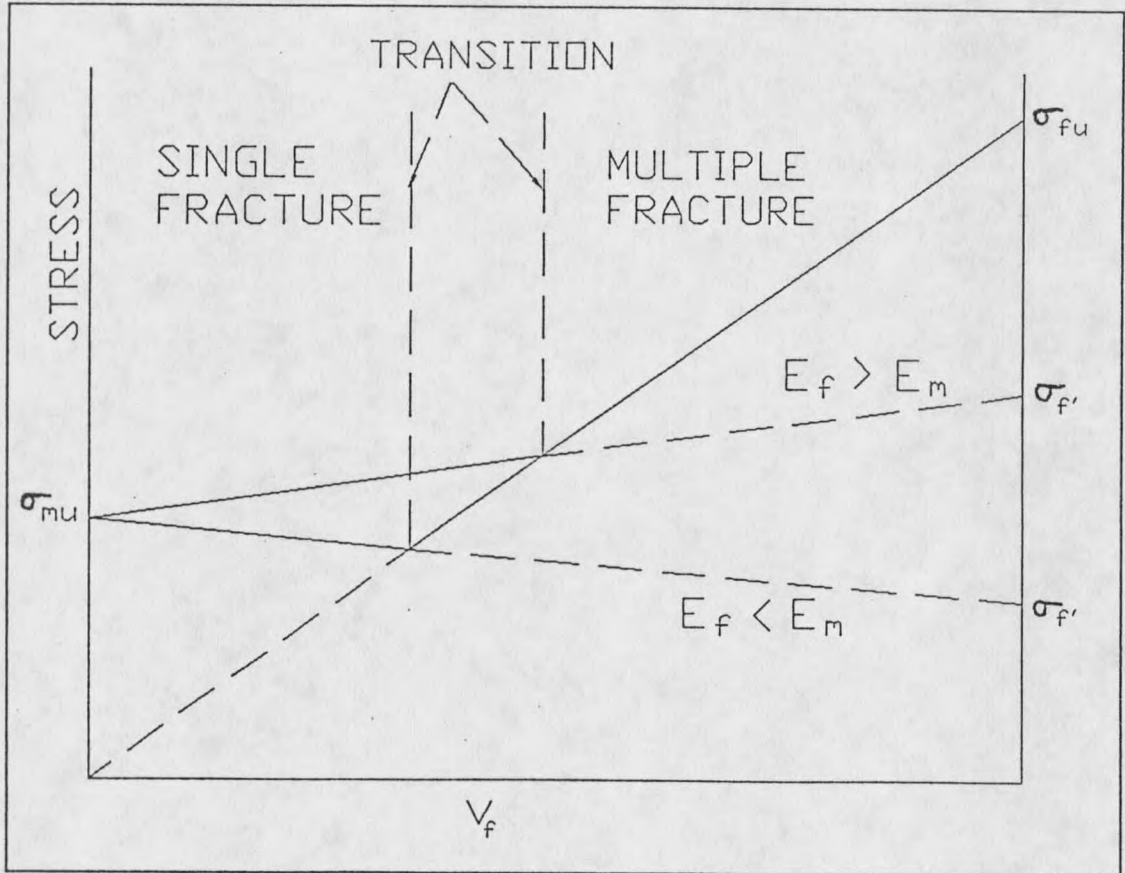


Fig.11 Transition from Single to Multiple Fracture as a Function of the Fiber Volume Fraction (adapted from 6)

All the terms are as explained before. This equation indicates that if the fiber diameter is reduced sufficiently, the effective cracking strain of a brittle matrix can be increased above its normal value, ϵ_{mu} . This effect has been reported to be observed experimentally (6), but is not widely proven.

This theory is applicable to some reinforced glasses and ceramics in which the fibers usually debond, and the shear stress at the interface is frictional sliding resistance as the matrix cracks open by sliding along the fibers. However, for many other composite systems, the interface is elastic and the stress transfer mechanism at the fiber-matrix interface is by elastic stress transfer. Aveston and Kelly (7) revised their first model to describe the cracking behavior for such composite systems. They employed a shear-lag analysis to explain this behavior. As explained earlier, the matrix cracking causes an additional load to be thrown onto the fibers. This additional load has a maximum value at the crack site and decreases away from the crack face, to approach zero. This stress transfer is given by the following expression.

$$\Delta\sigma = \Delta\sigma_0 \exp(-\sqrt{\phi}y) \quad \text{-----} \quad (2.15)$$

where

$$\phi = \frac{2G_m E_c}{(r^2 \ln(R/r) E_f E_m V_m)} \quad \text{-----} \quad (2.16)$$

As the load is increased, the matrix cracks into blocks of length between x and $2x$, where x is given by (7)

$$x = -\frac{1}{\sqrt{\Phi}} \ln \left[1 - \frac{\sigma_{mu} V_m}{\Delta \sigma_o V_m} \right] \text{ ----- (2.17)}$$

This equation indicates that the crack spacing decreases without limit provided that $\Delta \sigma_o$ may be increased without limit. This will not occur since the shear stress at the fiber-matrix interface is limited by the shear strength of the interface. As a result, some debonding takes place at the interface. The length of the fiber over which debonding takes place depends on the limiting shear stress at the interface after debonding has occurred. The limiting crack spacing for such a partially debonded case is given by (7)

$$L = \frac{r \Delta \sigma_o}{2\tau'} - \frac{1}{\sqrt{\Phi}} \left(\frac{\tau_u}{\tau'} + \ln \left[\frac{r\sqrt{\Phi} (\Delta \sigma_o - \sigma_{mu} V_m / V_f)}{2\tau_u} \right] \right) \text{ ----- (2.18)}$$

Multidirectional Composites

In these composites cracking begins in the off-axis plies with lowest strain to fracture. As loading continues, other off-axis plies crack. Crossplied (0/90) laminates are the most simple multidirectional laminate to consider. Considerable work has been done for crossplied polymer laminates, in which transverse cracking is observed at very low strain values. The behavior of this kind of laminate is similar to that of unidirectional CMC's, with the main difference that the longitudinal plies assume the role of the

fibers and the stress transfer now is across the interply interface instead of fiber-matrix interface. If the longitudinal plies are able to withstand the additional load thrown onto them, multiple cracking takes place in the transverse ply. In polymer matrices, longitudinal ply-matrix cracking is not observed. But in CMC's, longitudinal ply cracking follows the transverse cracking if the strain is increasing. If proper consideration is given to longitudinal ply matrix cracking and the ensuing stiffness reduction in the composite, the theories developed for polymer matrices may be applicable to CMC's. Hence the theoretical models developed for polymer-matrix composites are explained briefly in this section.

There are two approaches that can be used for analyzing the failure behavior of multidirectional laminates. One is the energy approach and the other is the fracture mechanics approach. The energy approach is the simpler of the two and is an extension of the theory developed for unidirectional composites by Aveston et.al. (7).

Strength Approach. Garret and Bailey (8) investigated transverse cracking in crossply laminates and the effects of transverse-ply thickness and applied stress on the resulting behavior. They based their theory on the shear-lag analysis, in which the plies remained elastically bonded. Glass fiber-reinforced epoxy crossply laminates were taken as the representative materials. After the first crack appeared in

the transverse ply, an additional load $\Delta\sigma$ is placed on the longitudinal ply. The value of this additional load is given by

$$\Delta\sigma = \Delta\sigma_0 \exp(-\sqrt{\phi}y) \text{ ----- (2.19)}$$

where

$$\phi = (E_c G_t) / (E_l E_t) * (b+d) / (bd^2)$$

They do not take into account the residual stresses and crack growth mechanisms. This theory has resulted in good correlation between the theory and the experiments in some cases.

Fracture Mechanics Approach. The simple strength approach assumes that the failure strength of the 90° ply is a lamina property, but this has been argued to be dependent on the laminate construction (10). Hence, this approach is rarely preferred to the fracture mechanics approach, in which it is assumed that a crack will propagate when the energy released by its formation is available. Two theories of interest are: (i) a self consistent scheme proposed by Laws and Dvorak (9), and (ii) variational approach by Nairn (10). Both the theories take residual stresses into account. The latter is more complicated, but both include the effects of the release of residual thermal strain energy due to the formation of microcracks. These two theories are explained briefly in this section and in the next chapter, with the necessary modifications added in this study to include the longitudinal

ply matrix cracking, so that the theories can be applied to CMC's of interest in the present work.

Simple Fracture Mechanics Model. This model is based on the hypothesis that a crack will propagate when it is energetically favorable to do so. The earlier proposed energy-based models assumed that the additional cracks occur at the midpoints between the existing cracks. This theory, on the other hand, can optionally consider that the location of the additional crack is associated with a probability density function, which is considered to be proportional to the stress in the transverse ply. The theory predicts explicit relationships between the loss of stiffness and the crack density and between the applied load and crack density. The loss of stiffness due to the transverse ply cracking is given as

$$E_{loss} = \left(1 + \frac{\beta}{\xi} \frac{dE_t}{bE_l} \tanh \frac{\xi}{\beta} \right)^{-1} \text{----- (2.20)}$$

where

- β = crack density parameter = thickness of the ply/crack spacing
- ξ = shear lag parameter
- E_t = modulus of transverse ply
- E_l = modulus of longitudinal ply
- b, d thickness of longitudinal and transverse plies respectively

The applied load for additional cracking is given as

$$\sigma_a = \left(\sigma_a^{fpf} + \frac{E_o}{E_t} \sigma_t^R \right) \left[2 \tanh \frac{\xi}{2\beta} - \tanh \frac{\xi}{\beta} \right]^{-1} - \frac{E_o}{E_t} \sigma_t^R \quad \text{-----} (2.21)$$

where

- σ_a^{fpf} = first failure stress of the transverse ply
- E_o = modulus of the composite
- σ_t^R = residual stress in the laminate

This theory is explained in more detail in the next chapter.

Variational Approach. This theory is built on the variational approach first proposed by Hashin (11,12). It includes the thermoelastic problem and an accurate calculation of the residual thermal stresses. All the earlier models were based on the shear-lag analysis model, which generally is based on the following assumptions (11):

- (a) the normal stress over the ply thickness is assumed to be constant.
- (b) the active area in which the shear stresses are assumed to be acting is supposed to be of unknown thickness in between the plies.
- (c) no interaction between the adjacent cracks.

These assumptions limit the accuracy of this kind of analysis. The more recent variational approach to solve the stiffness reduction and stress evaluation problem incorporates all the basic facts of the problem and has only one assumption (12): normal ply stresses are constant over the ply thickness in the direction of load. However, both theories assume that a large flaw already exists in the ply, and predict only the

conditions under which it will propagate. Additionally, both theories fail to consider the effects of the free (cut) edge of a specimen, where special stress concentrations exist; experimental data are taken for crack density only at the free edges, but appear generally similar to values in the interior (3). The model is based on the principle of minimum complementary energy and gives explicit relations between applied stress and crack density. Excellent agreement between the theory and experiments are reported for polymer matrices. With sufficient modification to include the effects of longitudinal ply matrix cracking, this theory is thought to be applicable to ceramic-matrix composites. This aspect is discussed in the next chapter.

CHAPTER 3

THEORY

Theoretical models are proposed here to explain the reported experimental behavior of laminates. These theoretical models are necessary to help in the design of these materials, so that catastrophic failure can be avoided. This is particularly true in the case of CMC's, for they retain a potential for brittle fracture at very low failure strains in some cases. Moreover, in the presence of cracks, oxygen, water and other substances enter the material, thus causing premature failures. Most of the composites are cooled down from higher manufacturing/solidification temperatures, as a result of which residual stresses are generated in the material, due to the thermal expansion mismatch between the matrix and the fibers. If these stresses are not taken into account, failure stress prediction will not be accurate enough in the design process.

The first step in this process is to understand the behavior of unidirectional composites. Then these ideas can be extended to much more practical composites with multidirectional reinforcement. The Aveston, Cooper and Kelly (5) theory gives an adequate approximation to the cracking behavior of unidirectional composites. They give the limiting crack spacing, the matrix failure strain and the resulting stiffness loss in the material.

Considerable attention has been given to the behavior of

crossplied polymer matrix composites. Existing theories describe the behavior of these composites quite adequately. However, this kind of attention has not been given the understanding of ceramic-matrix composites. If these materials are to be used in structural applications, a good theoretical model is necessary to predict their cracking behavior.

Two theoretical models are proposed in this thesis. They are built along the lines of the existing theoretical models for polymer-based matrices. Both the models are based on the fracture mechanics or energy release rate approach, according to which, a new microcrack will form when it is energetically favorable for it to propagate. Longitudinal ply matrix cracking is taken into consideration in both of the models. The classical theory of Aveston, Cooper and Kelly (7) is used for predicting matrix cracking in the longitudinal plies. The theoretical results are compared with the experimental results, obtained from the work done in a previous study (3), as described in the next chapter.

Predicted Behavior of CMC's Under a Tensile Load

As in any other types of cross-plyed laminates, cracking begins in the matrix/interfaces in the transverse ply. Accordingly, some load is transferred to the longitudinal ply. If the longitudinal ply can sustain this additional load, multiple cracking occurs in the transverse ply. These additional cracks are assumed to occur at the midpoints

between existing cracks. In most of the polymer-matrix composites that have been studied so far, this multiple cracking in the transverse ply continues until the longitudinal ply strength is exceeded or delamination occurs if the interply interface shear or peel stress exceeds the strength in that mode. The longitudinal plies do not undergo any cracking and, in fact, they inhibit the cracking in the adjacent transverse plies (6). However, in CMC's the matrix is very brittle and its breaking strain is very low. Hence the longitudinal ply matrix cracking follows the cracking in the 90° ply. This will reduce the stiffness of the 0° ply and hence of the composite. Also, the stress transfer from the longitudinal ply to the transverse ply is affected. Once the longitudinal ply cracking begins, it progresses very rapidly. This is shown in Fig.12. In Nicalon/1723, transverse ply cracking initiated at very low strain values (0.025 to 0.05%) (3). This was followed by the longitudinal ply matrix cracking at approximately 0.1% strain.

Models

Simple Fracture Mechanics Analysis -- Self-Consistent Scheme

This is an extension of the Laws and Dvorak shear lag based model (7). It is a good model in that it includes the effects of the residual stresses resulting from cool-down and thermal expansion mismatch. Moreover, there are no adjustable parameters except the non-dimensional shear lag

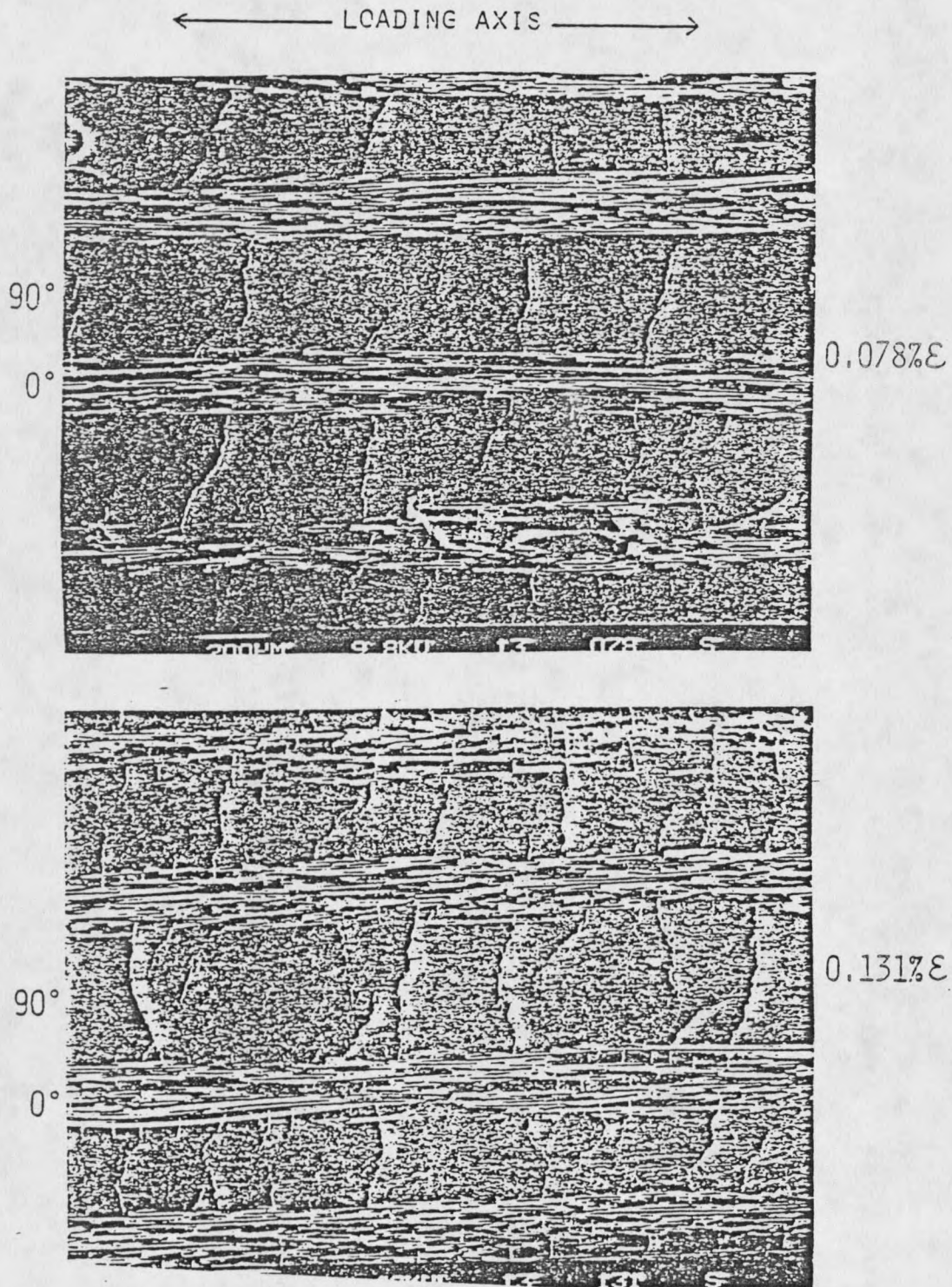


Fig.12 Cracking in the Transverse and Longitudinal Plies at Increasing Strain Levels (3)

← LOADING AXIS →

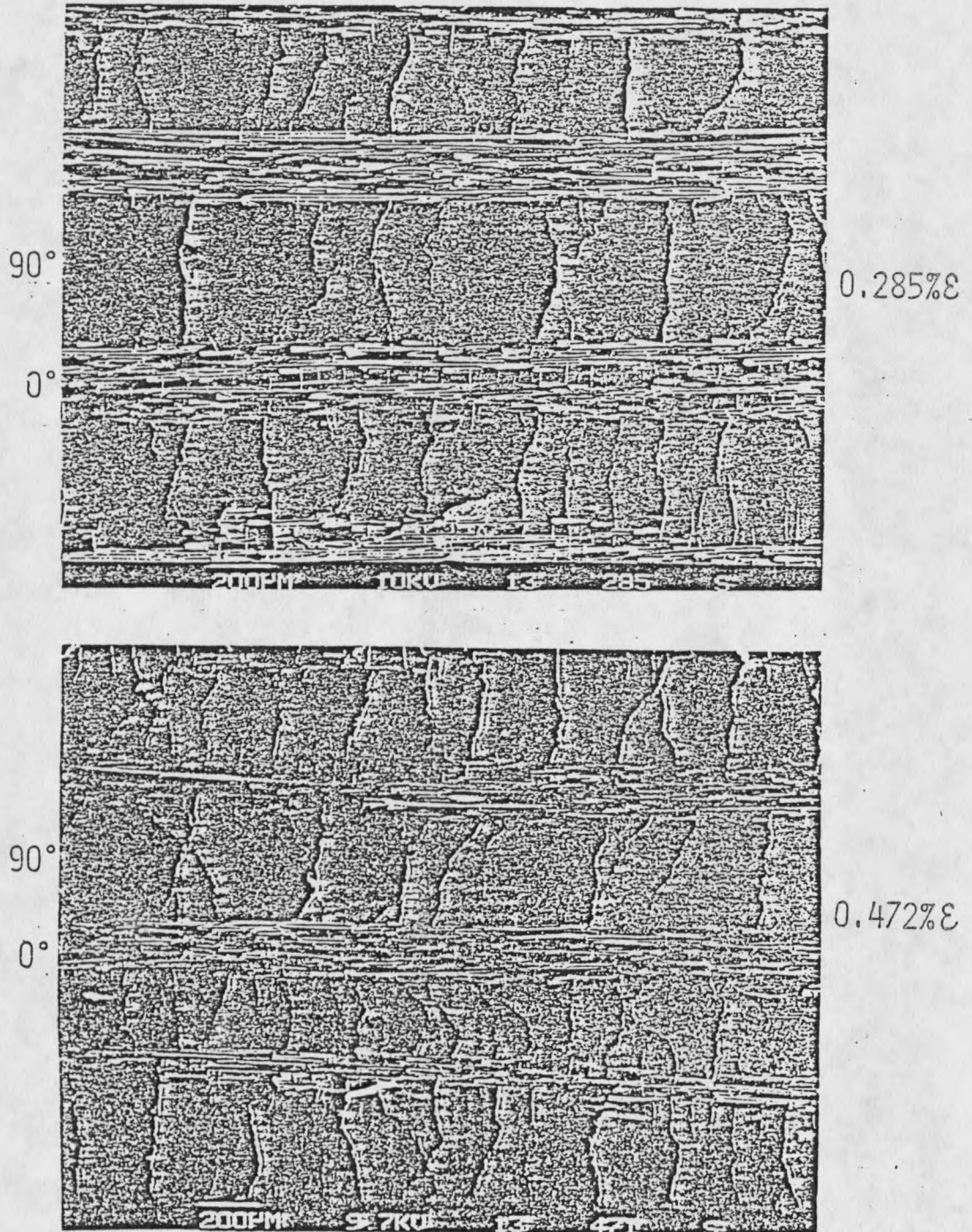


Fig.12 Continued...

parameter, which is curvefit using the data obtained from experiments and the stress on the composite. All other parameters are obtained from standard experiments. The theory also can consider the statistics of crack propagation in the sense that the position of the additional crack is calculated using the probability density function, which is assumed to be proportional to the applied stress. However, since the tensile stress in the 90° ply is maximum at the midpoint of the existing cracks, it is assumed here for simplicity that the additional crack occurs at the midpoints of the existing cracks, so that statistical effects in the original theory are not included. One parameter of significant value is the critical energy release rate- the amount of energy released due to the formation of a crack. This parameter has been evaluated in a concurrent study using the double-torsion technique (13).

Constitutive Equations. The laminate configuration used for this analysis is shown in Fig.13. This figure also shows the spacing of the two transverse cracks. Based on the laminate configuration, Laws and Dvorak found the stresses in the transverse and longitudinal plies as

$$\sigma_t = \left(\sigma_t^R + \frac{E_t}{E_o} \sigma_a \right) \left(1 - \frac{\cosh\left(\xi \frac{x}{d}\right)}{\cosh\left(\xi \frac{h}{d}\right)} \right) \text{-----} (3.1)$$

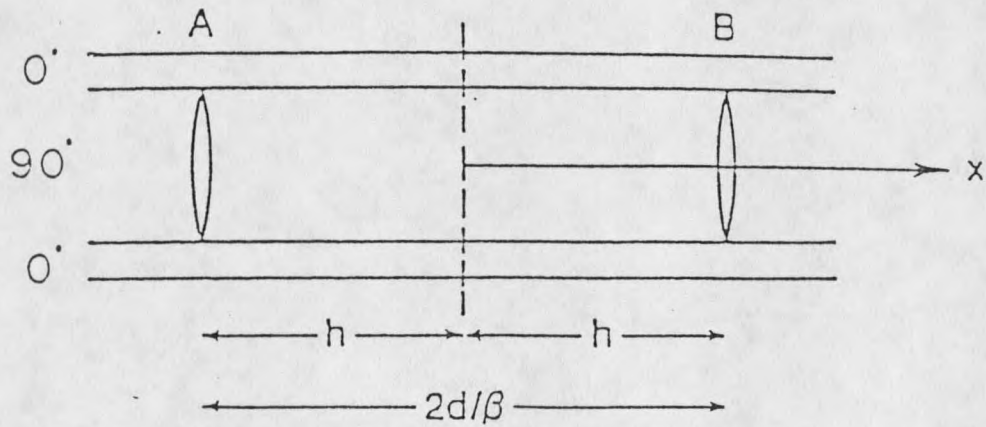
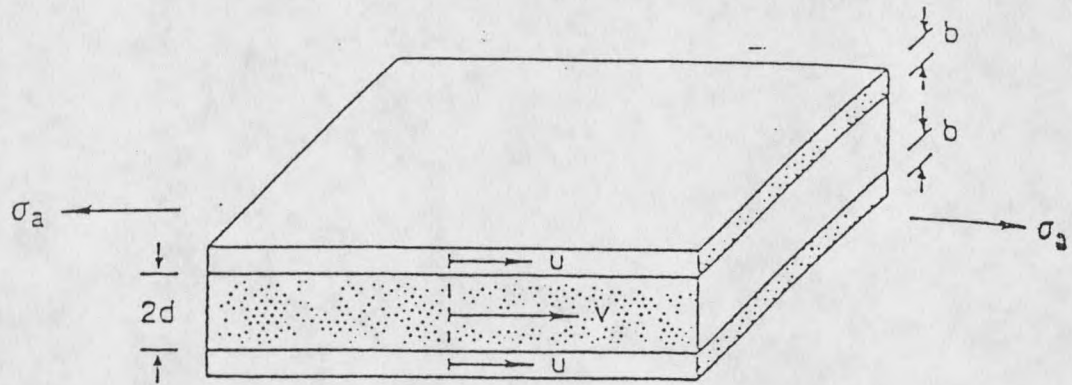


Fig.13 (a) Laws-Dvorak Analytical Model
 (b) Spacing of Two Transverse Cracks (9)

$$\sigma_1 = \frac{E_1}{E_o} \sigma_a \left(1 + \frac{dE_t}{bE_1} \frac{\cosh(\xi \frac{x}{d})}{\cosh(\xi \frac{h}{d})} \right) + \sigma_1^R \left(1 - \frac{\cosh(\xi \frac{x}{d})}{\cosh(\xi \frac{h}{d})} \right) \quad \text{----- (3.2)}$$

where

- σ_1^R = Residual thermal stress in the transverse ply
- σ_l^R = Residual thermal stress in the longitudinal ply
- E_t, E_l = modulus of the transverse and longitudinal plies respectively
- ξ = non-dimensional shear lag parameter
- b, d = thickness of the longitudinal and transverse plies respectively

As mentioned earlier, they used the simple shear lag theory for this purpose. The reduced stiffness due to transverse ply cracking is given as

$$E_o = \frac{E_o}{1 + \frac{\beta}{\xi} \frac{dE_t}{bE_1} \tanh\left(\frac{\xi}{\beta}\right)} \quad \text{----- (3.3)}$$

where β = crack density parameter = d/h .

This equation states that if there are no cracks in the transverse ply i.e., $\beta=0$, then $E=E_o$. On the other hand, if the crack density increases indefinitely i.e., $\beta=\text{inf}$, then $E=bE_l/(b+d)$, and the stiffness of the composite derives solely from the longitudinal ply and the transverse ply becomes ineffective.

As the load on the laminate is increased, the matrix in the longitudinal ply no longer can sustain the additional load shed to it, and it cracks. These are matrix cracks in the longitudinal ply, normal to the fibers, and are bridged by the reinforcing fibers. This cracking of the matrix results in a

stiffness reduction of the longitudinal ply, and consequently of the composite. The stiffness reduction in the 0^0 ply is given as (5)

$$E_{loss} = \frac{1}{\left(1 + \frac{\alpha}{2}\right) \left[2px' + \frac{1-2px'}{1 + \frac{\alpha}{2}} \right]} \quad \text{----- (3.4)}$$

where

$$\alpha = E_m V_m / E_f V_f$$

$$x' = (V_m / V_f) \sigma_{mu} r / 2\tau$$

E_m, E_f = matrix and fiber modulus respectively

V_m, V_f = matrix and fiber volume respectively

σ_{mu} = matrix failure stress

r = radius of the fiber

τ = fiber-matrix interface bond strength

The stiffness of the composite laminate can be found using classical laminate plate theory, but a large discrepancy was observed (3) between the experimentally measured moduli and the results calculated using the laminated plate theory. Hence, a corresponding reduction in the composite modulus was assumed to have taken place. The residual stresses and strains decline after matrix cracking initiates in the 0^0 ply (3). Hence these residual stresses were taken to be equal to zero in the limit. Due to the matrix cracking in the longitudinal ply, stress transfer between the 0^0 ply and the transverse ply decreases. This is exhibited in the value of the shear lag parameter. Its value decreases once the longitudinal ply cracking begins. However, this reduction in the shear lag parameter is more apparent during the first matrix cracking

due to the relaxation of residual stresses. After this, it reduces continuously but marginally.

The applied stress required for additional cracking in the transverse ply is given by

$$\sigma = \frac{(\sigma_a^{fpf} + \frac{E_o}{E_t} \sigma_t^R)}{\sqrt{(2 \tanh(\frac{\xi}{2\beta}) - \tanh(\frac{\xi}{\beta}))}} - \frac{E_o}{E_t} \sigma_t^R \quad \text{----- (3.5)}$$

where σ_a^{fpf} = first ply failure stress.

The effect of the longitudinal cracking on the applied stress is reflected in the composite modulus, which decreases in value as the cracking progresses, and the residual stress, which goes to zero as the longitudinal cracking progresses. The results of the above theory and comparison with the experimental results are given in the next chapter. Also, the applicability of the Aveston, Cooper and Kelly theory for the crossplied laminates is discussed in that chapter.

Variational Approach

Another recent analytical model for progressive transverse cracking that was found to be of interest was the one proposed by Nairn (10). This theory uses a much better stress analysis in analyzing the microcracking in the transverse plies than most of the existing energy release rate models, which use some form of shear lag approximation. The shear lag approximation is based on the fundamental assumption that there should be a large discrepancy in the stiffness of

the tensile load bearing components and the shear-stress transfer region, with the former being of much higher value (10). This kind of requirement is provided in unidirectional composites, in which the fibers (tensile load bearing components) are much stiffer than the matrix (shear-stress transfer region). But in a crossplied laminate, the stiffness of the 90° ply is not much greater than that of the matrix, and thus the shear-lag requirement is not fulfilled. Hence, it is postulated that shear-lag analysis will not give a quantitatively accurate solution (10). This necessitates a better theoretical model employing an improved stress analysis.

The present model is based on the variational analysis to calculate the strain energy release rate due to cracking. Also, it analyzes the residual thermal strain energy release as the microcracks form. The only explicit assumption this theory makes is that the x-axis tensile stresses in each ply are independent of the z-coordinate and depend only on the x-coordinate (Fig.14). As noted earlier, the theory does not include crack nucleation or free-edge effects.

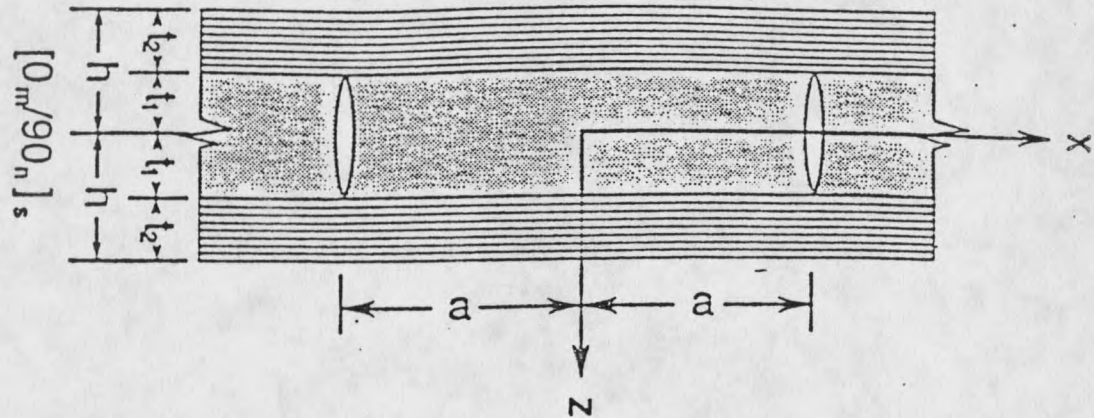


Fig.14 Geometry for Variational Analysis (10)

Constitutive Equations. The geometry used for the present analysis is shown in Fig.14. The admissible stress states which obey all stress equilibrium conditions, traction boundary conditions and interface continuity are given as (10)

$$\left. \begin{aligned} \sigma_x^{(1)} &= \sigma_{x0}^{(1)} - \psi(x); \\ \sigma_{xz}^{(1)} &= \psi'(x)z; \\ \sigma_z^{(1)} &= \frac{1}{2}\psi''(x)(ht_1 - z^2) \end{aligned} \right\} \text{----- (3.6a)}$$

$$\left. \begin{aligned} \sigma_x^{(2)} &= \sigma_{x0}^{(2)} + \frac{t_1}{t_2}\psi(x); \\ \sigma_{xz}^{(2)} &= \frac{t_1}{t_2}\psi'(x)(h-z); \\ \sigma_z^{(2)} &= \frac{t_1}{2t_2}\psi''(x)(h-z)^2 \end{aligned} \right\} \text{----- (3.6b)}$$

where the superscripts 1 and 2 denote the parameters in the transverse and longitudinal plies respectively, and the subscript 0 denotes the residual stress-free conditions.

The undetermined function $\psi(x)$ is found using the

principle of minimum complementary energy, according to which the minimum value for the complementary energy will give the best approximation to the composite strain energy. The function that is minimized is

$$\Gamma = \Gamma_0 + t_1^2 \int_{-1}^1 [C_1 \psi^2 + C_2 \psi \psi'' + C_3 \psi'^2 + C_4 \psi'^2 - 2\Delta \alpha T \psi + C_5 \psi''] d\xi \quad \text{----- (3.7)}$$

where

$$C_1 = \frac{hE_o}{t_2 E_L E_T}; \quad C_2 = \frac{\nu_T}{E_T} \left(\lambda + \frac{2}{3} \right) - \frac{\nu_L}{E_L} \frac{\lambda}{3}$$

$$C_3 = \frac{(\lambda+1)}{60 E_T} (3\lambda^2 + 12\lambda + 8); \quad C_4 = \frac{1}{3} \left(\frac{1}{G_T} + \frac{\lambda}{G_L} \right)$$

$$C_5 = \left(\alpha_T T - \frac{\nu_T \sigma_o}{E_o} \right) \left(\frac{2}{3} + \lambda \right) + \left(\alpha_T T - \frac{\nu_L \sigma_o}{E_o} \right) \frac{\lambda^2}{3}$$

and

$$\Gamma_o = \int_{-a}^a dx \int_0^{t_1} dz \left[\frac{\sigma_{xo}^{(1)2}}{E_T} + 2\alpha_T T \sigma_{xo}^{(1)} \right]$$

$$+ \int_{-a}^a dx \int_{t_1}^{h_1} dz \left[\frac{\sigma_{xo}^{(2)2}}{E_L} + 2\alpha_L T \sigma_{xo}^{(2)} \right]$$

$$l = a/t_1,$$

α_T, α_L = thermal expansion coefficients

$$\nu = \alpha_T - \alpha_L$$

$$\lambda = t_2/t_1$$

t_1, t_2 = thickness of the plies

G_L, G_T = shear moduli

ν_L, ν_T = Poisson's ratios

The subscripts L and T denote the axial and transverse ply

properties. Using the calculus of variations, the function $\psi(x)$ is found as

$$\psi = (\sigma_{x_0}^{(1)} - \frac{\Delta \alpha T}{C_1}) \Phi + \frac{\Delta \alpha T}{C_1} \text{-----} (3.8)$$

in which ϕ depends on the sign of $4q/p^2 - 1$

$$\Phi = \frac{2(\beta \sinh \alpha \rho \cos \beta \rho + \alpha \cosh \alpha \rho \sin \beta \rho)}{\beta \sinh 2\alpha \rho + \alpha \sin 2\beta \rho} \cosh \alpha \rho \cos \beta \rho + \frac{2(\beta \cosh \alpha \rho \sin \beta \rho - \alpha \sinh \alpha \rho \cos \beta \rho)}{\beta \sinh 2\alpha \rho + \alpha \sin 2\beta \rho} \sinh \alpha \rho \sin \beta \rho, \text{ for } \frac{4q}{p^2} > 1$$

$$\alpha = q^{\frac{1}{4}} \cos \frac{\theta}{2}$$

$$\beta = q^{\frac{1}{4}} \sin \frac{\theta}{2}$$

$$p = (C_2 - C_4) / C_3$$

$$q = C_1 / C_3$$

$$\phi = \frac{\beta \cosh \alpha \xi}{\sinh \alpha \rho (\beta \coth \alpha \rho - \alpha \coth \beta \rho)} + \frac{\alpha \cosh \beta \xi}{\sinh \beta \rho (\alpha \coth \beta \rho - \beta \coth \alpha \rho)}, \text{ for } \frac{4q}{p^2} < 1$$

$$\alpha = \sqrt{\frac{-p}{2} + \sqrt{\frac{p^2}{4} - q}}$$

$$\beta = \sqrt{\frac{-p}{2} - \sqrt{\frac{p^2}{4} - q}}$$

The above equations completely describe the thermoelastic stress state. The additional crack occurs at the midpoint of the existing cracks where the stress is maximum. The energy release rate for the formation of the new crack is

given as

$$G_c = \left(\sigma_o^2 \frac{E_T^2}{E_o^2} + \frac{\Delta \alpha^2 T^2}{C_1^2} \right) t_1 C_3 [2\chi(\rho/2) - \chi(\rho)] \quad \text{----- (3.9)}$$

in which the value of χ depends on the sign of $4q/p^2$

$$\chi(\rho) = 2\alpha\beta(\alpha^2 + \beta^2) \frac{\cosh(2\alpha\rho) - \cos(2\beta\rho)}{\beta \sinh(2\alpha\rho) + \alpha \sin(2\beta\rho)}, \quad \text{for } \frac{4q}{p^2} > 1$$

and

$$\chi(\rho) = \alpha\beta(\beta^2 - \alpha^2) \frac{\tanh(\beta\rho) \tanh(\alpha\rho)}{\beta \tanh(\beta\rho) - \alpha \tanh(\alpha\rho)}, \quad \text{for } \frac{4q}{p^2} < 1$$

As a result of this cracking in the transverse ply, the stiffness of the composite decreases. Hence, the compliance, which is reciprocal to the stiffness, increases. This compliance is given as

$$C = \frac{L}{2hE_oW} + \frac{E_T^2 t_1 C_3 L}{2E_o^2 h^2 W} \frac{\sum \chi(\rho_i)}{\sum \rho_i} \quad \text{----- (3.10)}$$

where L and W are length and width of the laminate.

As the cracking in the transverse plies progresses, the load on the composite increases continuously and the longitudinal ply matrix cracking may initiate at some strain. The behavior of the longitudinal ply is similar to that explained before for unidirectional composites. The matrix cracks are bridged by the reinforcing fibers. As a result of this matrix cracking, the stiffness of the longitudinal ply and hence of the composite decreases. This might result in

reduced stress transfer between the longitudinal and transverse plies, which might in turn inhibit the cracking in the transverse ply. The reduction in the stiffness of the longitudinal ply is again given by the equation (7)

$$E_{loss} = \frac{1}{\left(1 + \frac{\alpha}{2}\right) \left[2px' + \frac{(1-2px')}{\left(1 + \frac{\alpha}{2}\right)}\right]} \quad \text{----- (3.11)}$$

The various parameters are the same as explained before. A corresponding reduction in the composite stiffness was assumed to have occurred. The applied stress for further cracking and the resulting stiffness loss have been calculated. The analytical results are compared with the results obtained from the experiments. This is explained in the ensuing chapter.

CHAPTER 4

RESULTS AND DISCUSSION

The applicability of a theoretical model is determined by comparing the results obtained using the theory with those obtained from experiments. If the results compare well with the experimental values, the analytical model is said to predict the failure behavior of a material quite adequately. This method of comparison is based on the assumption that the experimental measurements are accurate. Thus, an analytical model to predict the behavior of a material can only be validated within the accuracy of the test methods used to determine the experimental values. Moreover, the model should be broad enough to be applicable to a set or class of similar materials. This verification can be done by applying the developed theoretical model to different materials, which exhibit similar behavior. In the present work, two models are developed to predict the behavior of ceramic matrix composites. Their applicability is determined by comparing predictions with experimental data from Ref.3 for (i) the applied stress vs. crack density in the transverse ply (ii) the applied stress vs. crack density in the longitudinal ply (iii) stiffness loss vs. crack density.

The Aveston, Cooper and Kelly model (7) was used to include the longitudinal ply matrix cracking effect, which has not been done in previous studies. This theory was separately verified with the experimental values, as discussed in the

following sections.

Applicability of the ACK Model

The ACK theory was used in this work to account for the longitudinal ply matrix cracking. The fiber-matrix bond strengths were measured previously and are given in Table 1. The residual stresses due to thermal expansion mismatch are taken into consideration, as can be seen from the table.

TABLE 1

Average Bond Strengths
Nicalon Fiber-Reinforced Glass and Glass-Ceramics (3,16,17)

Composite System	τ_{deb} (MPa)		
	Thermal Residual	Mechanical	Mechanical + Residual
Nicalon/1723	-31.16	236	204.84
Nicalon/CAS-I	-24.59	249	224.41
Nicalon/CAS-IIb	-22.48	204	181.52
Nicalon/BMAS-III	45.70	60	105.70
Nicalon/LAS-III	63.11	56	119.11

These bond strengths are dominated by the interphase carbon layer which forms upon processing (3). Lithium aluminosilicate and Barium magnesium silicate matrices have low thermal expansion coefficients. This causes radial residual tensile stresses to develop at the fiber-matrix interface upon cooling from higher manufacturing temperatures (3). In the other two

materials, compressive radial residual stresses are reported to form.

The ACK theory was basically developed to explain the behavior of unidirectional composites. It considers the case of brittle matrices, like ceramics, with fibers having higher breaking strains than the matrix. In the crossplied composites that are of interest in the present work, the matrix cracking of the longitudinal plies is precipitated by the additional load thrown onto them upon the transverse ply cracking. Other than that, their behavior is thought to be similar to that of unidirectional laminates. Hence the ACK theory was first checked with experimental values obtained for unidirectional laminates. These experimental values were again taken from Ref.3.

As explained in Chapter 3, the ACK theory gives the stiffness loss in a unidirectional laminate due to matrix cracking. This stiffness loss is a function of the crack density. With these values of stiffness and crack density, the applied stress was determined. This was plotted against applied strain. The applied stress vs. applied strain curve was then plotted against experimental values. This is shown in Figures 15 and 16. The analytical results agree fairly well with those obtained from standard experiments. This comparison shows that the values used for the fiber-matrix interface bond strength are accurate enough. The use of this theory for the case of multiple longitudinal ply matrix cracking in a cross-

plied composite is discussed in the later part of this section.

Results for the Self-Consistent Scheme

The property data used for the present analysis are given in the Appendix A. The critical energy release rate, an important parameter in the fracture mechanics analysis, was experimentally found using the double-torsion technique (13). The applied stress, using the equations discussed earlier in chapter 3, was found using various values of crack density - the crack density parameter (ply thickness/crack spacing) was varied from .1 to 4 in steps of .1 for the transverse ply. The size of the steps was varied for the longitudinal ply to obtain the best agreement with experimental data, as described later. This wide range of crack densities was considered to give a good relationship between applied stress and crack density. A computer code was written for this purpose. The flow diagram for this computer program is given in the Appendix B and the code itself is given in Appendix C. These values of applied stress were plotted against the crack density in the transverse ply. When the applied stress reached a certain value at which the matrix in the longitudinal ply starts cracking, a reduction in the stiffness of the longitudinal ply and hence in the composite was introduced. These values were then compared with the experimental values. This is shown in Figures 17 - 19. The point at which the

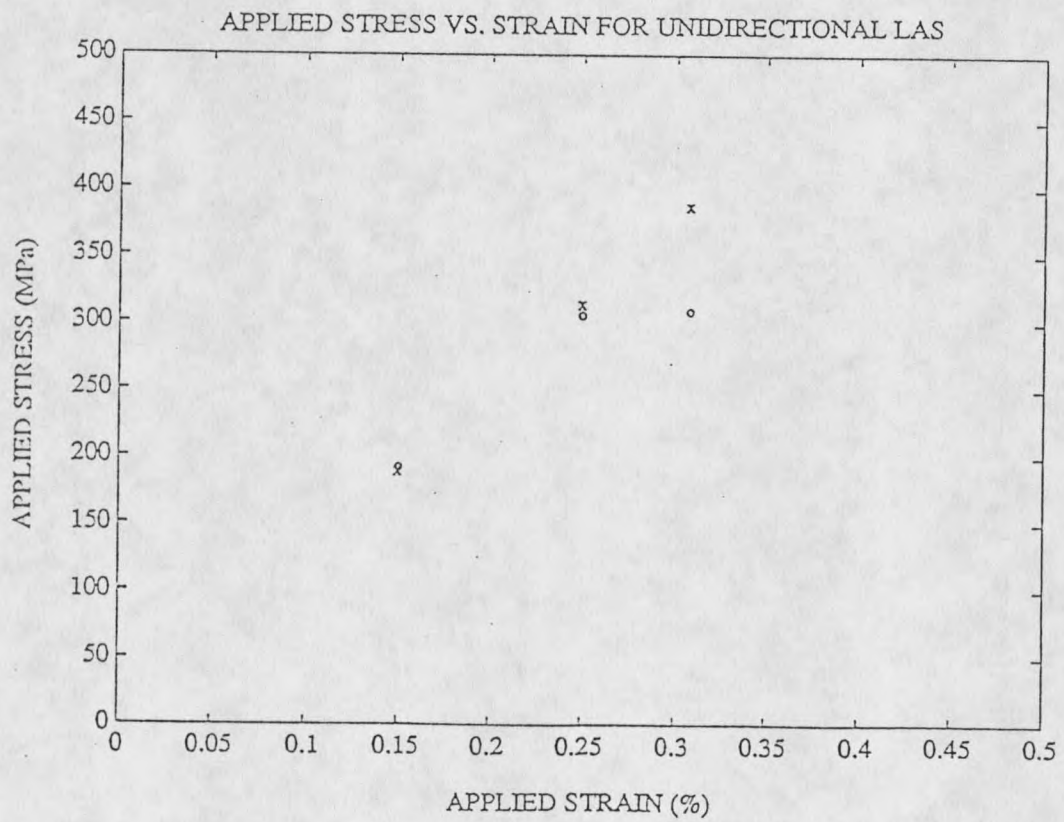


Fig.15 Applied Stress Vs. Strain for Unidirectional Nicalon/1723. Experimental Values (o) from Ref.3

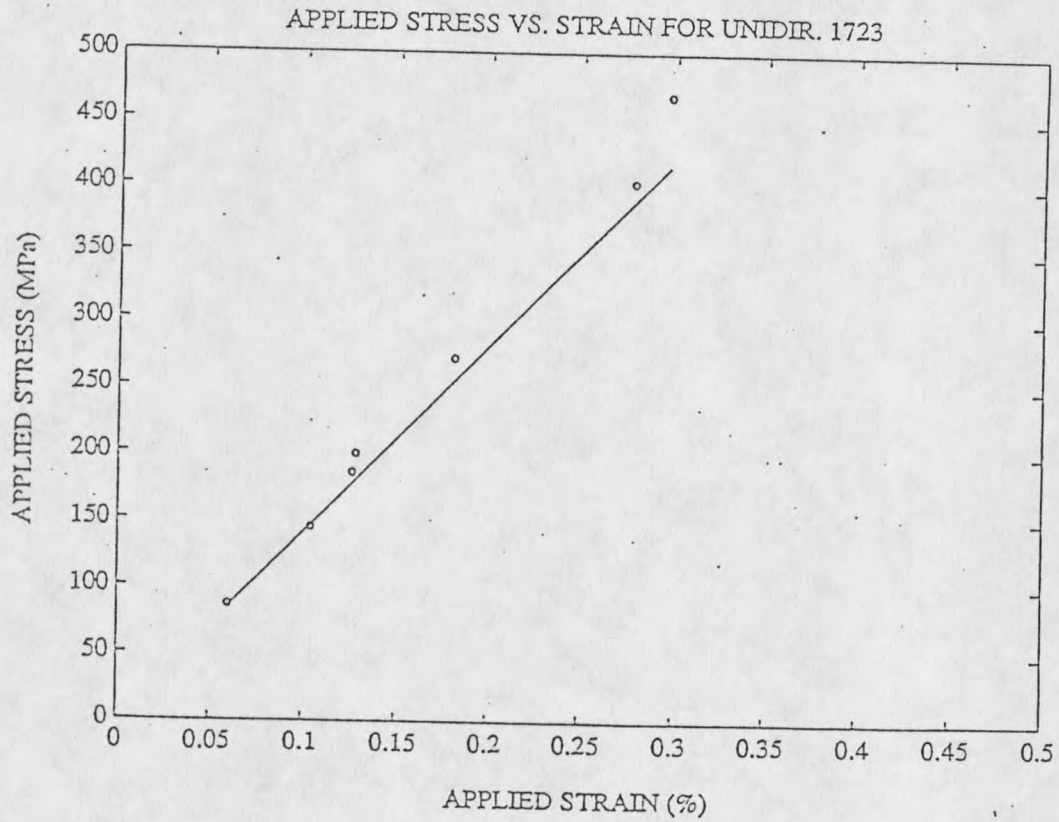


Fig.16 Applied Stress Vs. Strain for Unidirectional Nicalon/LAS. (x) -- Theoretical Predictions; (o) -- Experimental Values (3)

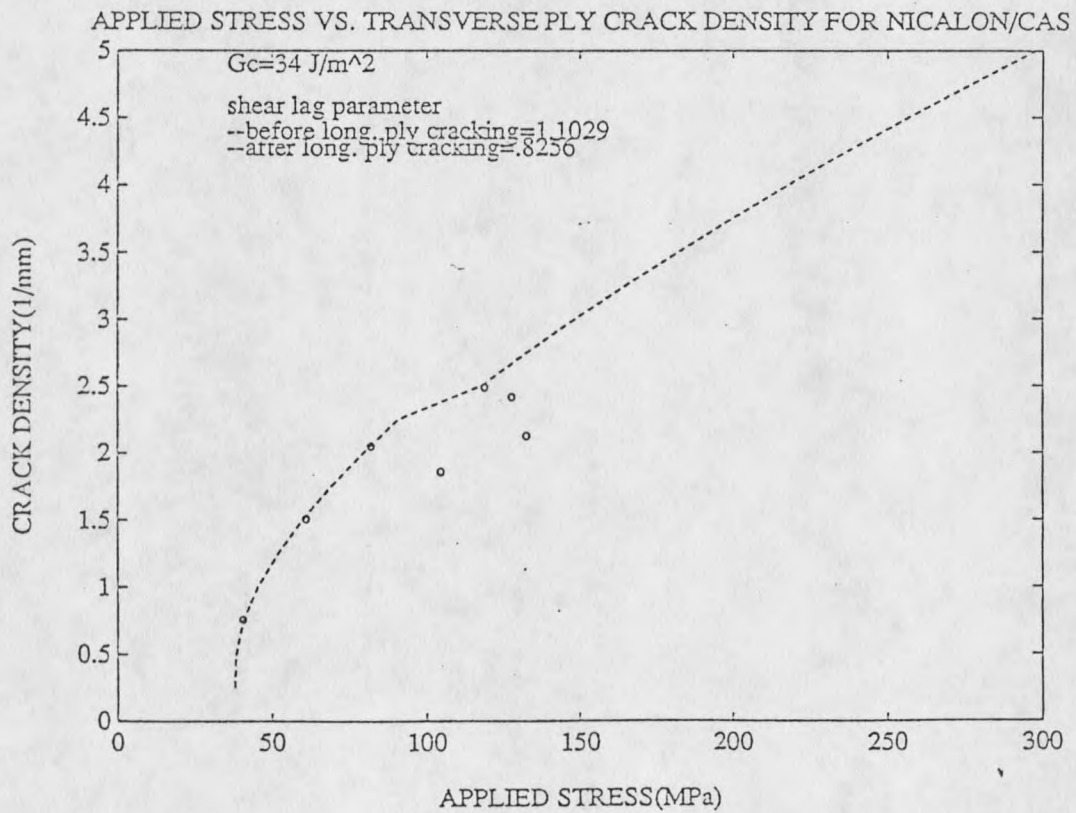


Fig.17 Applied Stress Vs. Transverse Ply Crack Density for Nicalon/CAS Using Modified Laws and Dvorak Theory. Experimental Values (o) from Ref.3

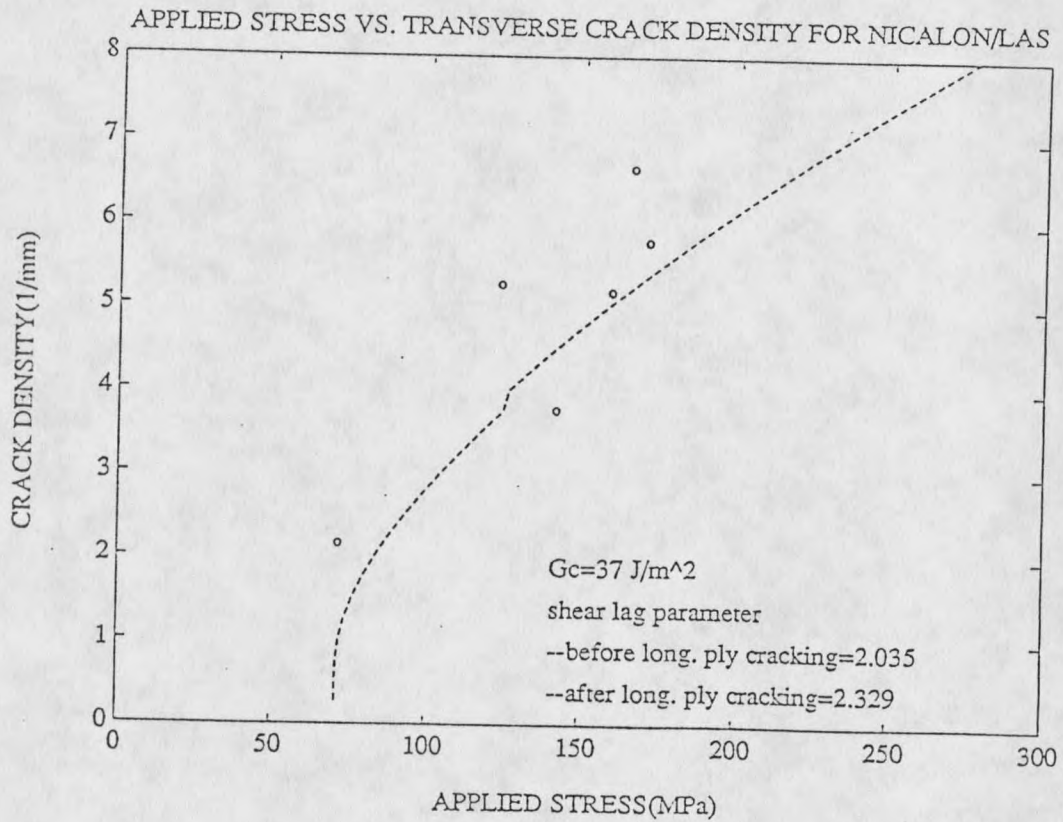


Fig.18 Applied Stress Vs. Transverse Ply Crack Density for Nicalon/LAS Using Modified Laws and Dvorak Theory. Experimental Values (o) from Ref.3

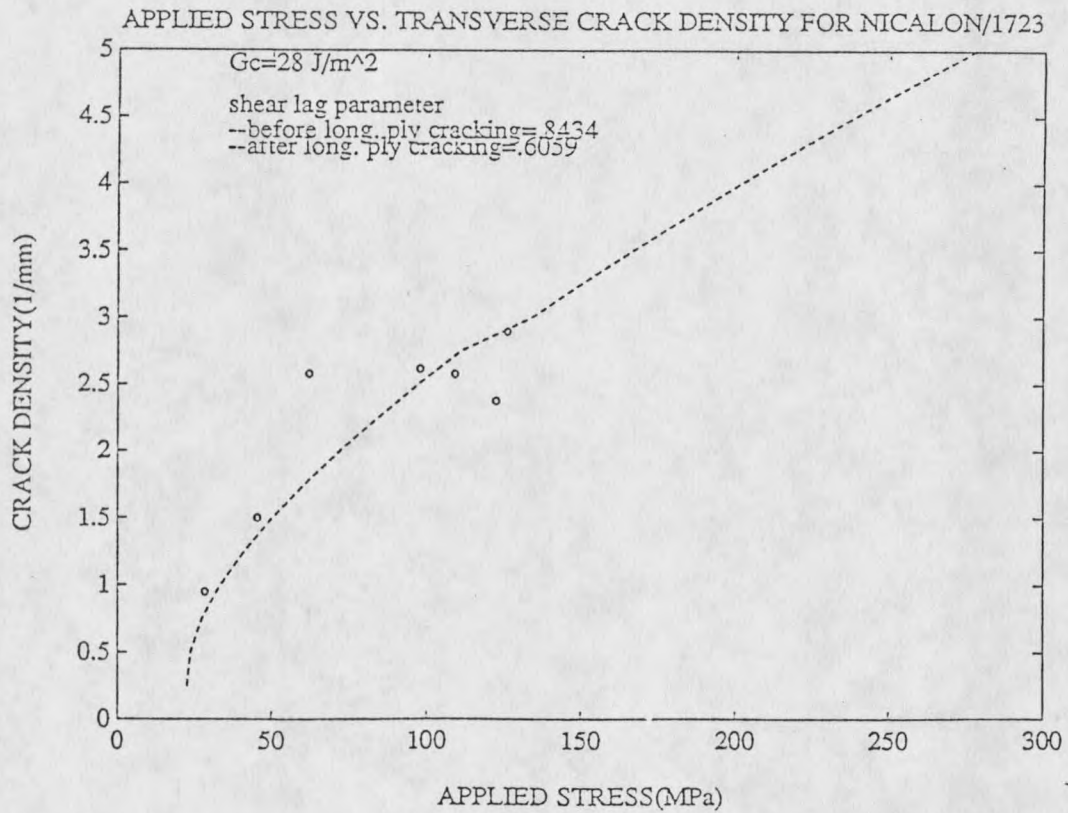


Fig.19 Applied Stress Vs. Transverse Ply Crack Density for Nicalon/1723 Using Modified Laws and Dvorak Theory. Experimental Values (o) from Ref.3

longitudinal ply matrix cracking begins is shown by the discontinuity in the curve. It is encouraging to note that the analytical results are in good agreement with those obtained from experiments.

The applied stress vs. crack density in the longitudinal ply is also plotted and compared with the experimental values. A wide range of values of crack density parameter (thickness of the ply/crack spacing) was selected to give the best fit of the predicted longitudinal matrix crack density to the experimental data. The longitudinal crack density was taken to be a fixed multiple of the transverse ply crack density above the stress where longitudinal ply matrix cracking was calculated to occur. For the CAS, LAS and 1723 matrices, the best fit was obtained for longitudinal to transverse ply crack densities of 4:1, 3:1, and 6:1 respectively. These are in the general range found experimentally (3), and shown in the micrographs in Fig.12. The results are shown in Figures 20-22.

Due to matrix cracking first in the transverse ply and then in the longitudinal ply, the stiffness of the plies and hence of the composite reduces dramatically. This might effectively cause structural failure in some applications. Thus, an analytical model describing the failure behavior of a material is not complete unless it predicts stiffness behavior of the material. This theory gives an explicit expression for the stiffness loss as a function of the crack

density. The ratio of the reduced modulus to the original modulus value is plotted against the crack density in Figures 23-25. The theory predicts that the modulus reduces very sharply in the beginning, but as the transverse crack density reaches a saturation level, about 3 to 4 cracks per mm, the stiffness stabilizes. However, the experimental data show that the modulus reduces even after this. This may be attributed to the fact that the residual stresses in the laminate are assumed to go to zero upon the onset of longitudinal ply matrix cracking. In reality, these residual stresses decrease gradually as the cracking progresses in the longitudinal ply. Further work should be done to consider this gradual decrease in the residual stresses. The experimental data for the modulus may also be questionable, as broad scatter is evident.

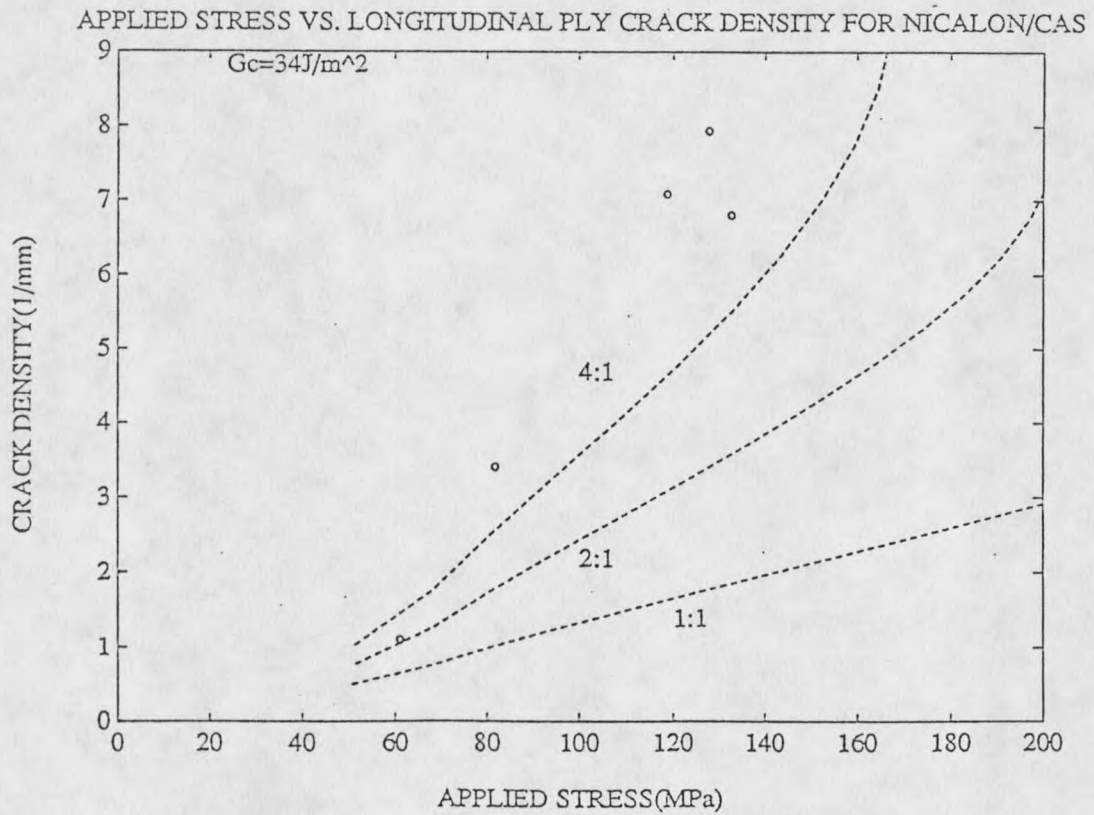


Fig.20 Applied Stress Vs. Longitudinal Ply Crack Density for Nicalon/CAS Using Modified Laws and Dvorak Theory. Experimental Values (o) from Ref.3. The Ratio Shown is Between the Step Sizes of Longitudinal Ply Crack Density Parameter and That of the Transverse Ply.

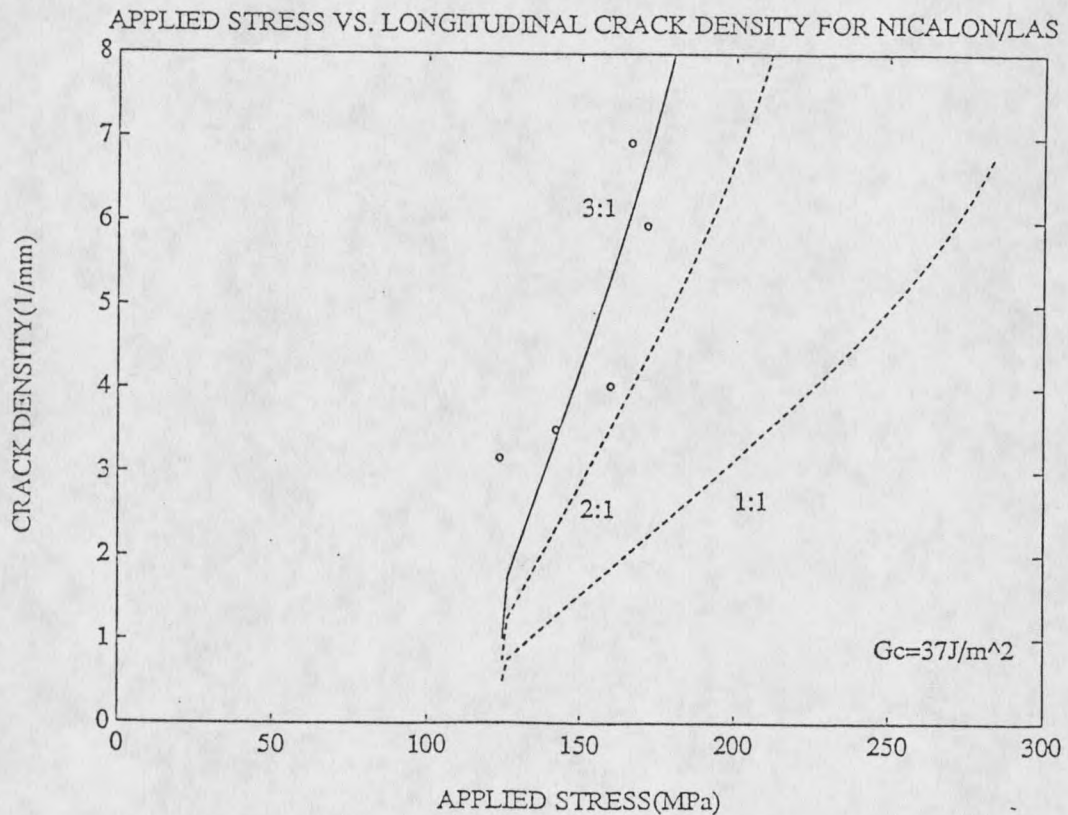


Fig.21 Applied Stress Vs. Longitudinal Ply Crack Density for Nicalon/LAS Using Modified Laws and Dvorak Theory. Experimental Values (o) from Ref.3. The Ratio Shown is Between the Step Sizes of Longitudinal Ply Crack Density Parameter and That of the Transverse Ply.

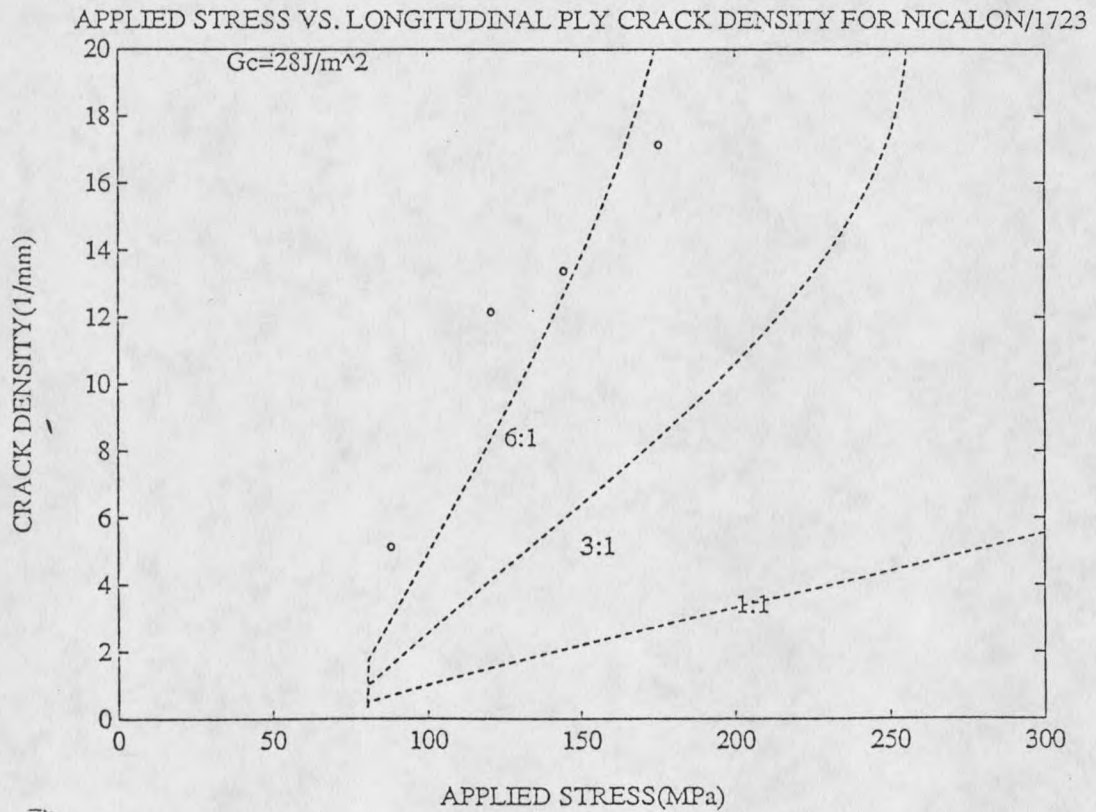


Fig.22 Applied Stress Vs. Longitudinal Ply Crack Density for Nicalon/1723 Using Modified Laws and Dvorak Theory. Experimental Values (o) from Ref.3. The Ratio Shown is Between the Step Sizes of Longitudinal Ply Crack Density Parameter and That of the Transverse Ply.

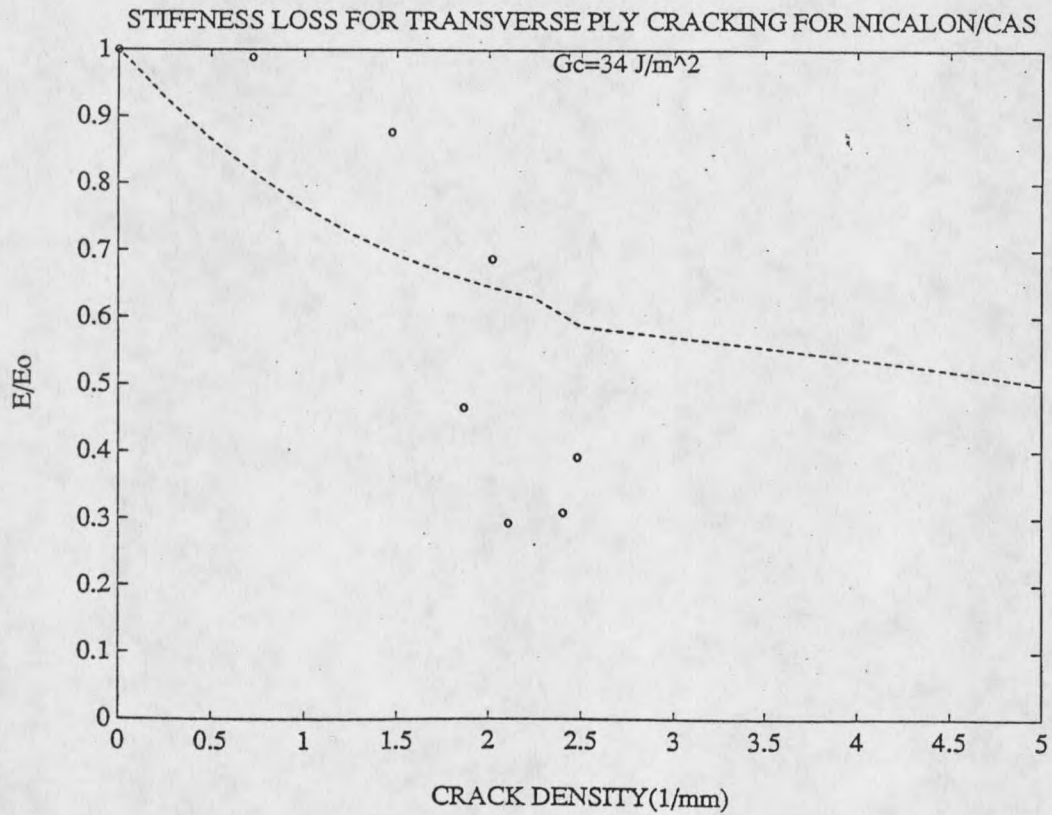


Fig.23 Comparison of Theoretical and Experimental Stiffness Loss for Crossplied Nicalon/CAS. Experimental Values (o) from Ref.3. Uses Modified Laws and Dvorak Theory

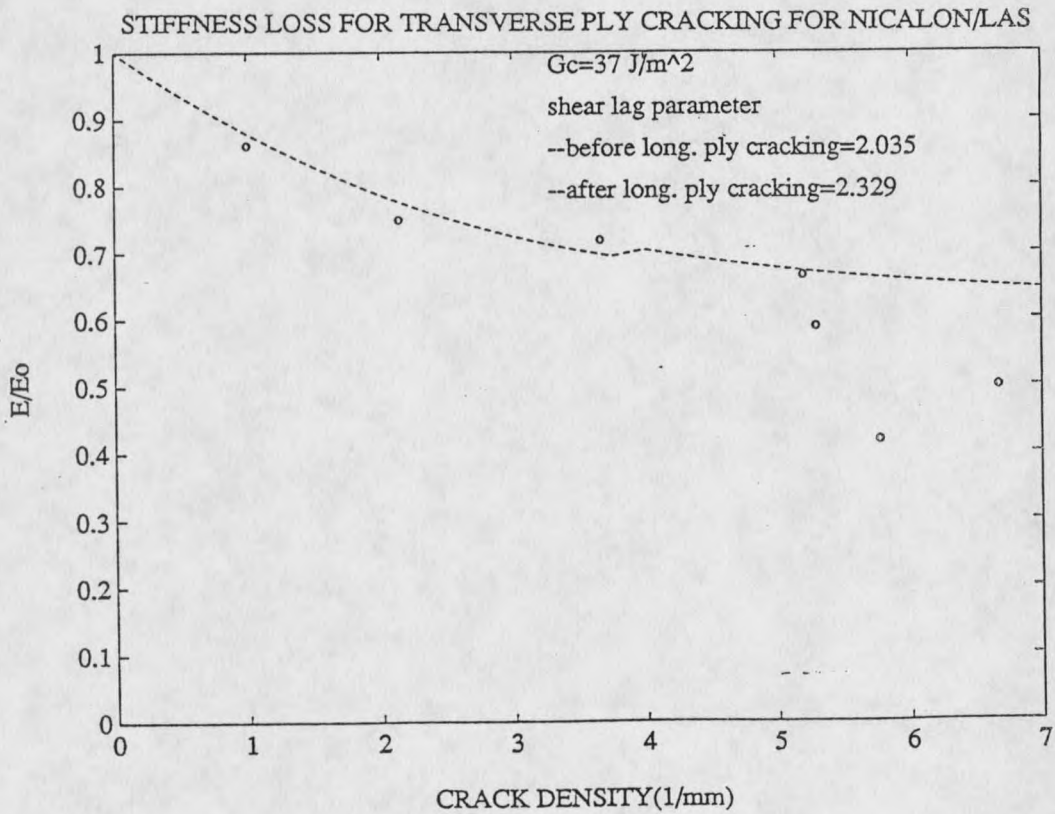


Fig.24 Comparison of Theoretical and Experimental Stiffness Loss for Crossplied Nicalon/LAS. Experimental Values (o) from Ref.3. Uses Modified Laws and Dvorak Theory

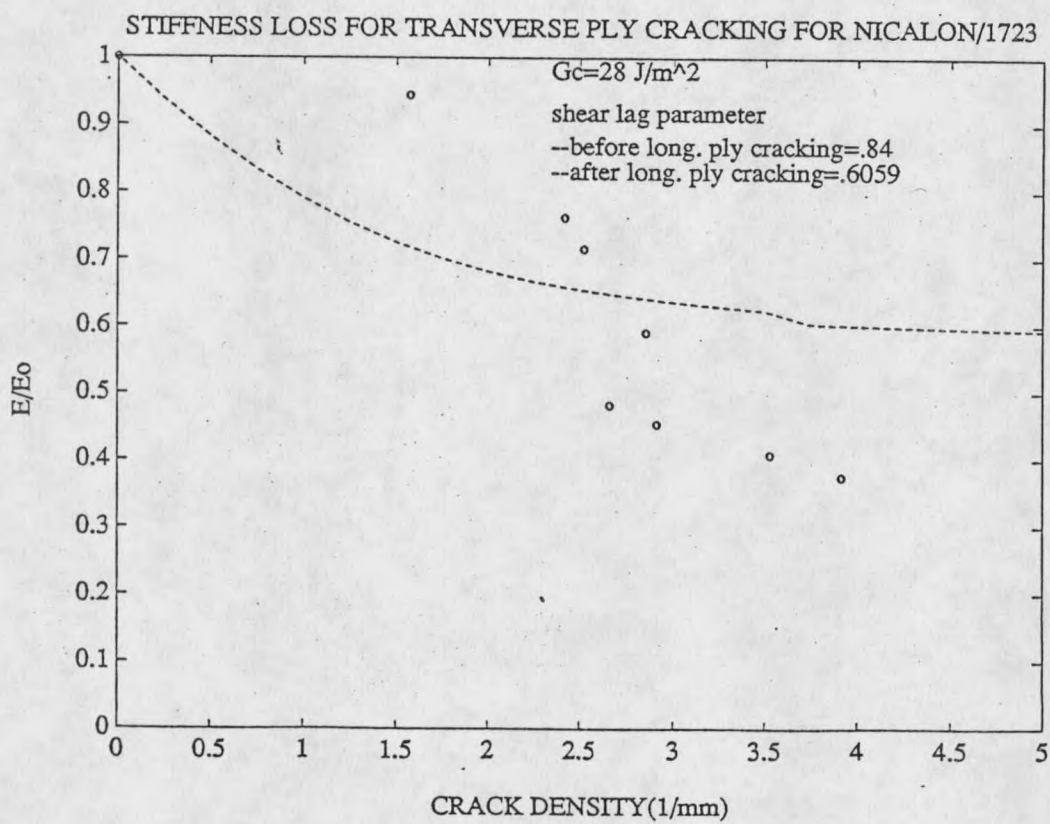


Fig.25 Comparison of Theoretical and Experimental Stiffness Loss for Crossplied Nicalon/1723. Experimental Values (o) from Ref.3. Uses Modified Laws and Dvorak Theory

Results for the Variational Analysis

This theory is based on a stress analysis which does not use the shear-lag theory. There are no adjustable parameters in the sense that all the parameters that are used in this theory are found from standard experiments. Hence, any agreement between this theory and experiment is more impressive due to the absence of curve-fitting parameters. In this case also, the applied stress needed to cause cracking in the transverse ply was plotted against crack densities. Again, a wide range of crack densities was selected to give a good relationship between the applied stress and crack density and stiffness loss and crack density. These results are compared with the experimental values. This is shown in Figures 26-27. The computer code used for these calculations is given in Appendix D. Agreement here is less good than for the previous theory although the theory does pass through the data with no curve fitting, it does not accurately follow the trendline of the data or capture the initial cracking points at low stress.

The stiffness loss resulting due to matrix cracking in the plies was also plotted against the crack density and is shown in Figures 28 and 29. Correlation of theory and experiment here is again difficult due to the experimental data scatter.

Comparison of the Two Theories

Both theories are able to simulate the cracking data to some extent. The modified Laws and Dvorak model predicts lower first ply failure stress in the transverse ply, which agrees with the experimental data. Also, the effect of the onset of longitudinal ply matrix cracking can be clearly seen on the applied stress vs. crack density plot in this theory. Although the modified Nairn model predicts higher first ply failure stress, the theory is in reasonable agreement with the data over much of the stress range. This is remarkable since there were no parameters that were curvefit in this model, unlike in the shear lag analysis, where the shear lag parameter was curvefit using the experimental data. The results using both the theories for Nicalon/CAS is shown in Fig.30a.

Stiffness predictions were similar in both of the theories. Again, the stiffness comparison is not very meaningful due to the scatter in the experimental values.

Both of these theories employ more defensible assumptions as compared with the limited earlier attempt in Ref.3 (see Fig.30), and the Laws and Dvorak theory gives an improved fit to the data. The earlier work did not consider the progressive interaction of cracking in the transverse and longitudinal plies. Also, measured values for G_c were not available at that time, and those calculated from first ply cracking were significantly too low, thus shifting the rest of

the shear lag parameters. This is further discussed in the conclusions section.

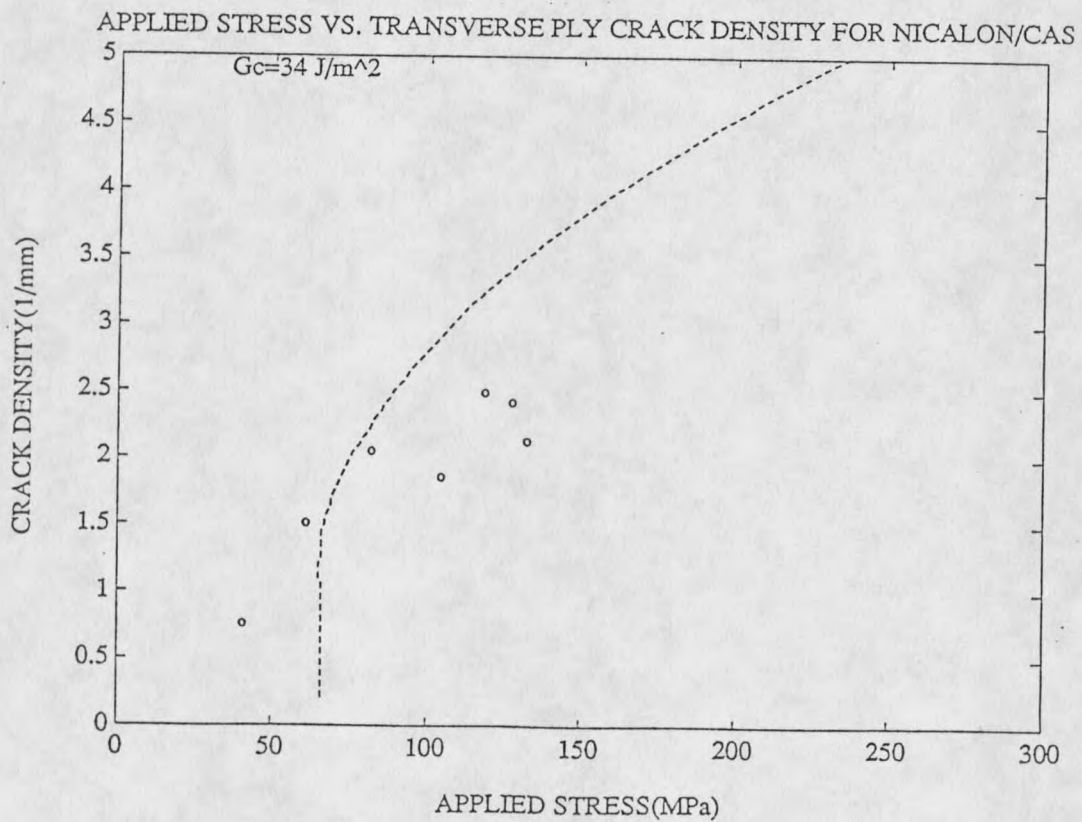


Fig.26 Applied Stress Vs. Transverse Crack Density for Nicalon/CAS Using Modified Nairn's Analysis. Experimental Values (o) from Ref.3

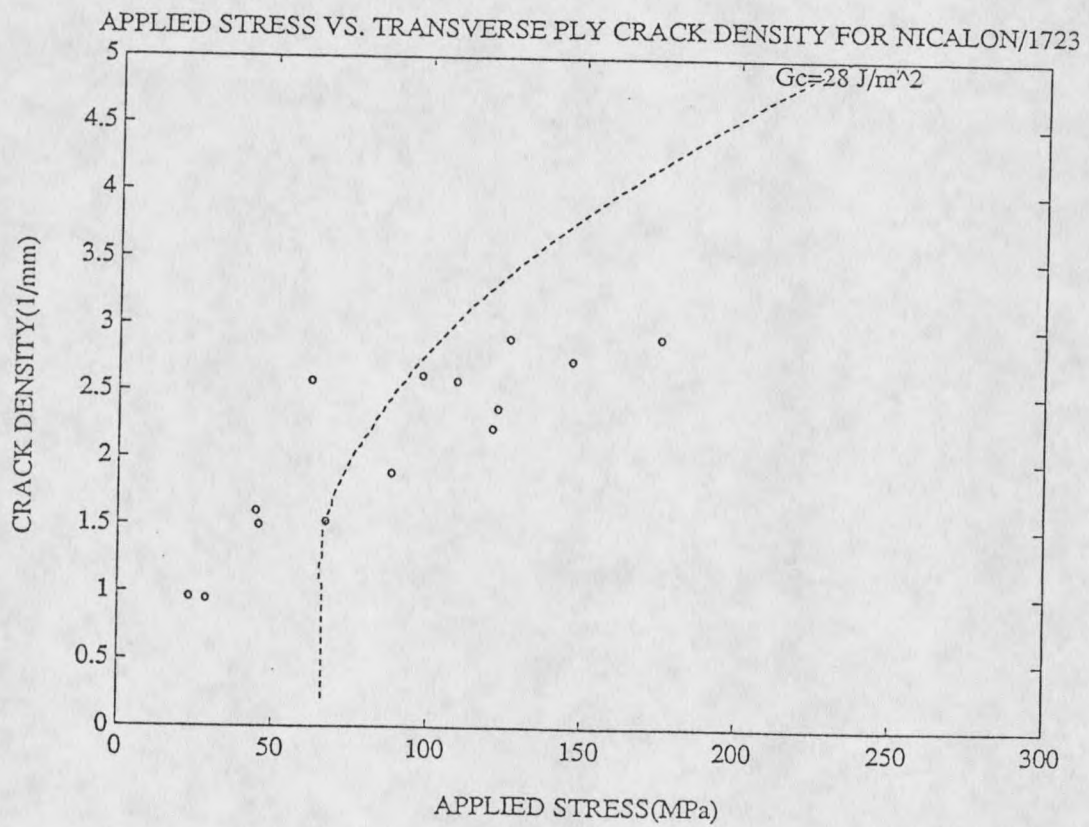


Fig.27 Applied Stress Vs. Transverse Crack Density for Nicalon/1723 Using Modified Nairn's Analysis. Experimental Values (o) from Ref.3

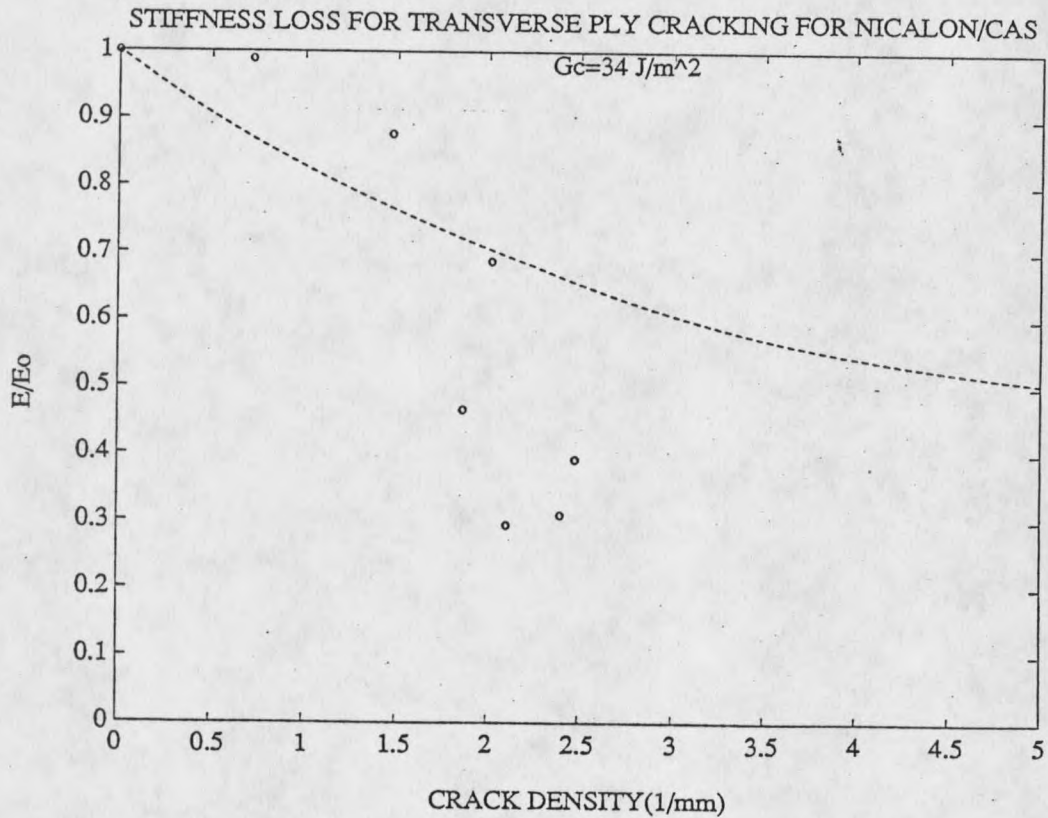


Fig.28 Theoretical Stiffness Loss Vs. Experimental Stiffness Loss (o) Using Modified Nairn's Analysis. Experimental Values from Ref.3; Nicalon/CAS

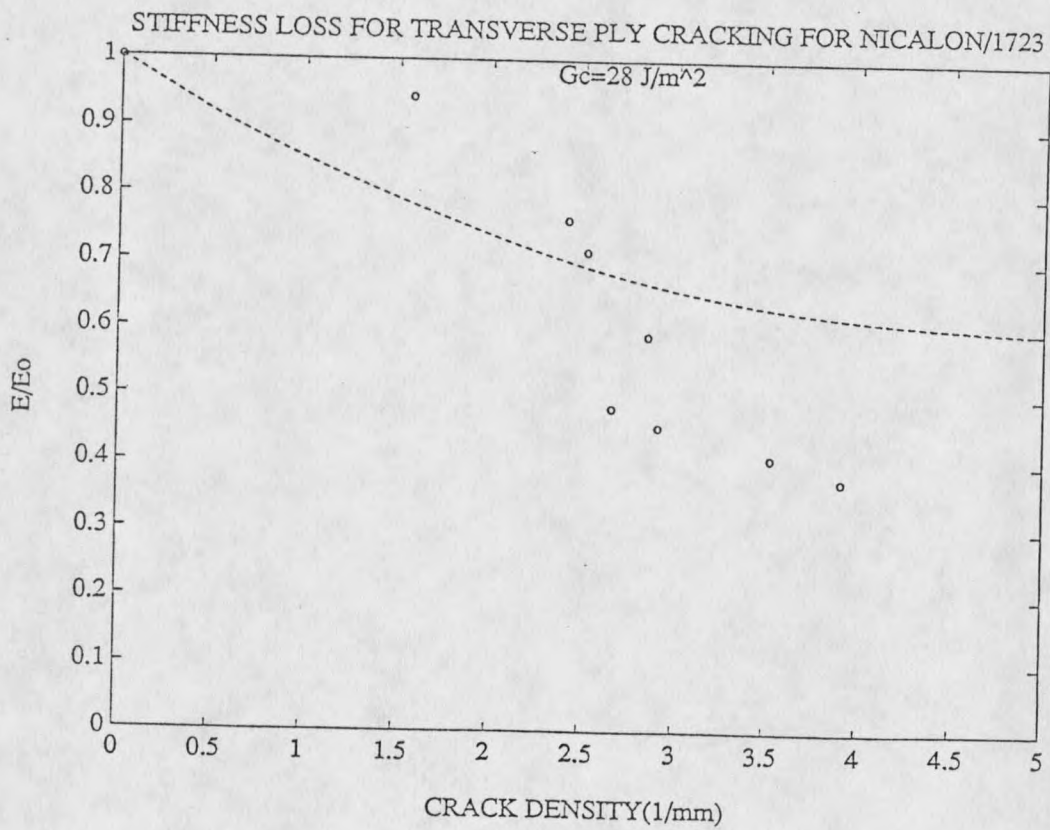


Fig.29 Theoretical Stiffness Loss Vs. Experimental Stiffness Loss (o) Using Modified Nairn's Analysis. Experimental Values from Ref.3; Nicalon/1723

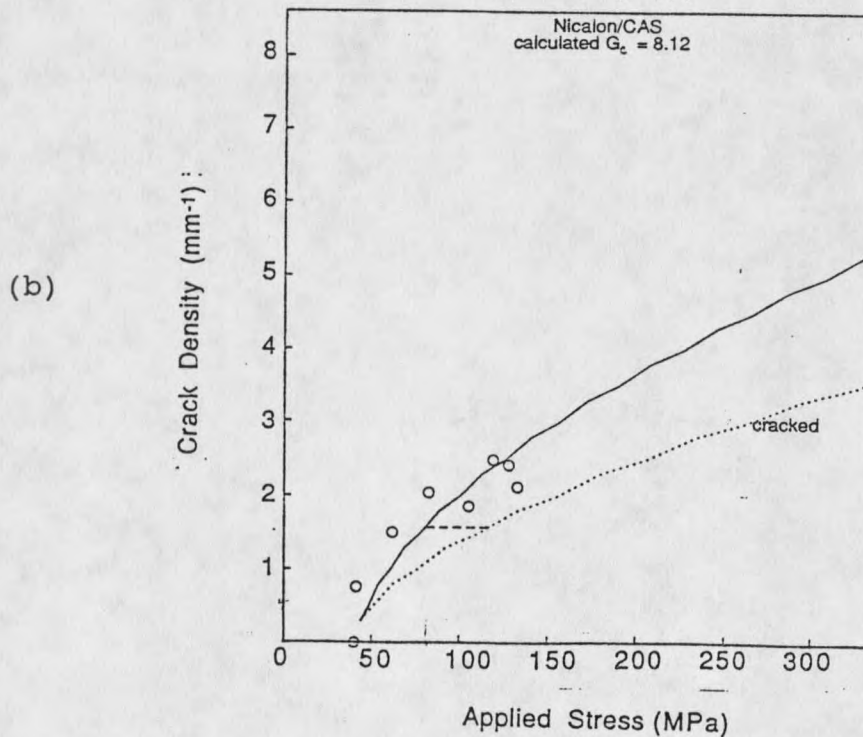
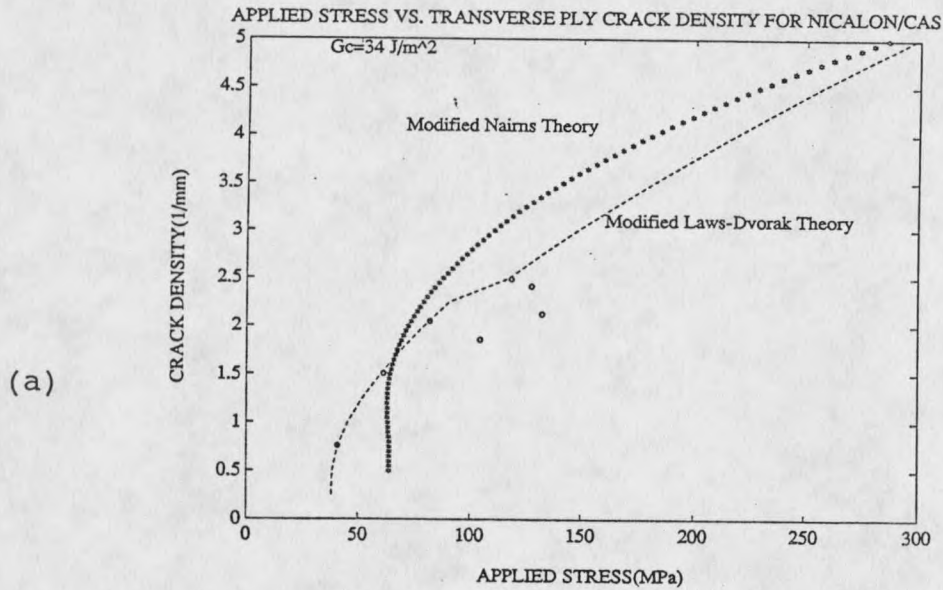


Fig.30 (a) Applied Stress Vs. Transverse Ply Crack Density for Nicalon/CAS, Using Modified Laws-Dvorak Theory (-), Modified Nairn's Theory (*) and Experimental Values (o) (b) Similar Plot using Earlier Developed Theory (3)

CHAPTER 5

CONCLUSIONS AND RECOMMENDATIONS FOR FURTHER WORK

Conclusions

The main objective of the present work was to improve theoretical modelling of cross-ply ceramic-matrix composites. To assure broad applicability of this model, three materials of Nicalon-reinforced ceramic-matrix laminates were considered as representative materials. These materials have different thermal expansion coefficients and thus had varying residual stresses. This helped in the study of residual stress and fiber-matrix interface bond strength effects on the cracking behavior of these materials.

Two theoretical models are developed to explain the behavior of a CMC. These models were developed on the lines of the existing models based on polymer-matrices. Good agreement is shown between the analytical results and the experimental results, particularly for the Laws and Dvorak model. From this, it can be concluded that if sufficient modification is done to account for longitudinal ply matrix cracking, the models based on the polymer matrices can work as well for CMC's. The stiffness properties were also studied. The study showed that the stiffness stabilizes as the crack density reaches a saturation level, but agreement with experimental data was uncertain due to scatter in the data.

The effect of including the longitudinal ply cracking in

the analysis was studied as a main parameter. It was found that there wasn't much effect till the crack density in this ply reached a high value. This may be due to the fact that these cracks are bridged by the fibers, which can still carry a significant amount of load. Of the two theories developed in this work, it is concluded that the method based on the variational analysis is more rigorous in the sense that it considers the problem of cracking with no curve fit parameter. However, the Laws and Dvorak model provided a better fit to the experimental data for crack density.

Comparison with the Earlier Developed Theory

In an earlier developed theory (3), the applied stress was computed as a function of crack density and the results were plotted for two cases: (i) no cracks in the longitudinal ply and (ii) preexisting cracks in the longitudinal ply. The Laws and Dvorak model was modified for this purpose. In the second case, a 5% reduction in the stiffness of the longitudinal ply and the composite was assumed. The results are shown in Fig.30. Due to the lack of experimental value for fracture surface energy, G_c , this value was calculated using Hahn's analysis (18). These values of G_c were found to be very low as compared to the experimental values (10). Comparing that theory with the present Laws and Dvorak theory, it can be seen that better correlation is found in the present study.

Recommendations

Much of the modelling done is applicable for room-temperature behavior of the CMC's. If these materials are to be used for high temperature structural applications, a theoretical model to predict the design stresses at elevated temperatures has to be developed. The value of fracture toughness was calculated at room temperature. More work has to be done to calculate this value at elevated temperatures, if these materials are to be designed for high temperature use. Due to the lack of any relationship between the applied stress and the number of cracks in the longitudinal ply, an arbitrary number of cracks were considered in this ply, for each crack in the transverse ply, to get the best fit with the experimental data for applied stress vs. longitudinal ply crack density. Thus, there is a need for improved data in this area.

Most of the theories developed so far consider crossplied composites. Consideration must be given to more general angle plies. Also, edge effects should be studied. Residual stresses decline as a result of cracking in the plies. An extensive treatment of this area must be carried out, since residual stresses play an important role in CMC's. Finally, more work has to be done to analyze the fracture processes microscopically for better designing of these materials. Interfaces between the different plies must be studied to understand the behavior of these composites. Finite

element analysis or a more rigorous classical mechanics model may be useful for this purpose.

REFERENCES CITED

REFERENCES CITED

- (1) Robert R. Irving, "Researchers Seeking New Ways to Make Ceramics Less Brittle, Longer Lasting", Metalworking News, June 20, 1988
- (2) Salvatore J. Grisaffe, "Ceramic-Matrix Composites", Advanced Materials and Processes, vol.137, issue 1, pp.43-44 and 93-94 Jan'90
- (3) K.A. Danneman, "Damage Development and Failure of Fiber-Reinforced Ceramic Matrix Composites", Ph.D. Thesis, Massachusetts Institute of Technology, Dept. of Materials Science and Engineering, Cambridge, MA (1989)
- (4) John F. Mandell, "Glass and Ceramic-Matrix Composites", Course Notes (1990)
- (5) J. Aveston, G.A. Cooper and A. Kelly, "Single and Multiple Fracture", The Properties of Fiber Composites, Conf. Proceedings, National Physics Lab, pp. 15-26, Nov 4'71
- (6) J.B. Morley, "Growth of Matrix Cracks in Brittle Matrix Composites", High Performance Composites, Academic Press Ltd., London, 1981
- (7) J. Aveston and A. Kelly, "Theory of Multiple Fracture of Fibrous Composites", Journal of Mat. Sci., 8 (1973) pp. 352-362
- (8) K.W. Garret, J.E. Bailey, "Multiple Transverse Fracture in 90° Cross-ply Laminates of a Glass Fibre-Reinforced Polyester", Journal of Mat. Sci., 12 (1977), pp. 157-168
- (9) Norman Laws and George J. Dvorak, "Progressive Cracking in Composite Laminates", Journal of Com. Mat., vol.22, pp.900-916, oct'88
- (10) John A. Nairn, "The Strain Energy Release Rate of Composite Microcracking: A Variational Approach", Journal of Com. Mat., vol 23, pp. 1106-1129, Nov'89
- (11) Hashin Z., "Analysis of Cracked Laminates: A Variational Approach", Mechanics of Materials 4 (1985), pp. 121-136
- (12) Hashin Z., "Analysis of Stiffness Reduction of Cracked Cross-ply Laminates", Engineering Fracture Mechanics vol 25, Nos 5/6, pp.771-778, 1986
- (13) J.B. Schutz, "Failure Criteria for Ceramic-Matrix Composites", Ph.D. Thesis, Massachusetts Institute of Technology, Dept. of Materials Science and Engineering,

Cambridge, MA (1990)

(14) D.Hull, "An Introduction to Composite Materials", Cambridge University Press, Cambridge, 1981.

(15) P.K.Mallick, "Fiber-Reinforced Composites", Marcel Dekker, INC., New York, 1988

(16) D.H.Grande, "Testing and Properties of High Temperature Glass-Ceramic Matrix Composites", Ph.D. Thesis, Massachusetts Institute of Technology, Dept. of Materials Science and Engineering, Cambridge, MA (1987).

(17) D.H.Grande, J.F.Mandell and K.C.C.Hong, "Fiber/Matrix Bond Strength Studies of Glass, Ceramic and Metal Matrix Composites", J.Mat.Sci., 23 (1), pp. 311-328 (1988)

(18) Y.M.Han, H.T.Hahn and R.B.Croman, "A Simplified Analysis of Transverse Ply Cracking in Cross-ply Laminates", Comp. Sci. and Tech., 31, pp.65-177 (1988)

APPENDICES

Appendix A
Parameters for the Model (3)

NICALON/1723

$b=d$	=	0.2 mm
E_l	=	140.6 GPa
E_t	=	101.0 GPa
E_o	=	103.04 GPa
G_{23}	=	45.82 GPa
α_{lm}	=	$4.30 \times 10^{-6} / ^\circ C$
σ_{R^m}	=	+13.59 MPa
σ_{R^t}	=	-13.59 MPa
σ_{R^l}	=	0.0158 %
ϵ_{tpf}	=	0.026 % (exptl)
σ_a	=	22.64 MPa (exptl)
G_c	=	34 J/m ²

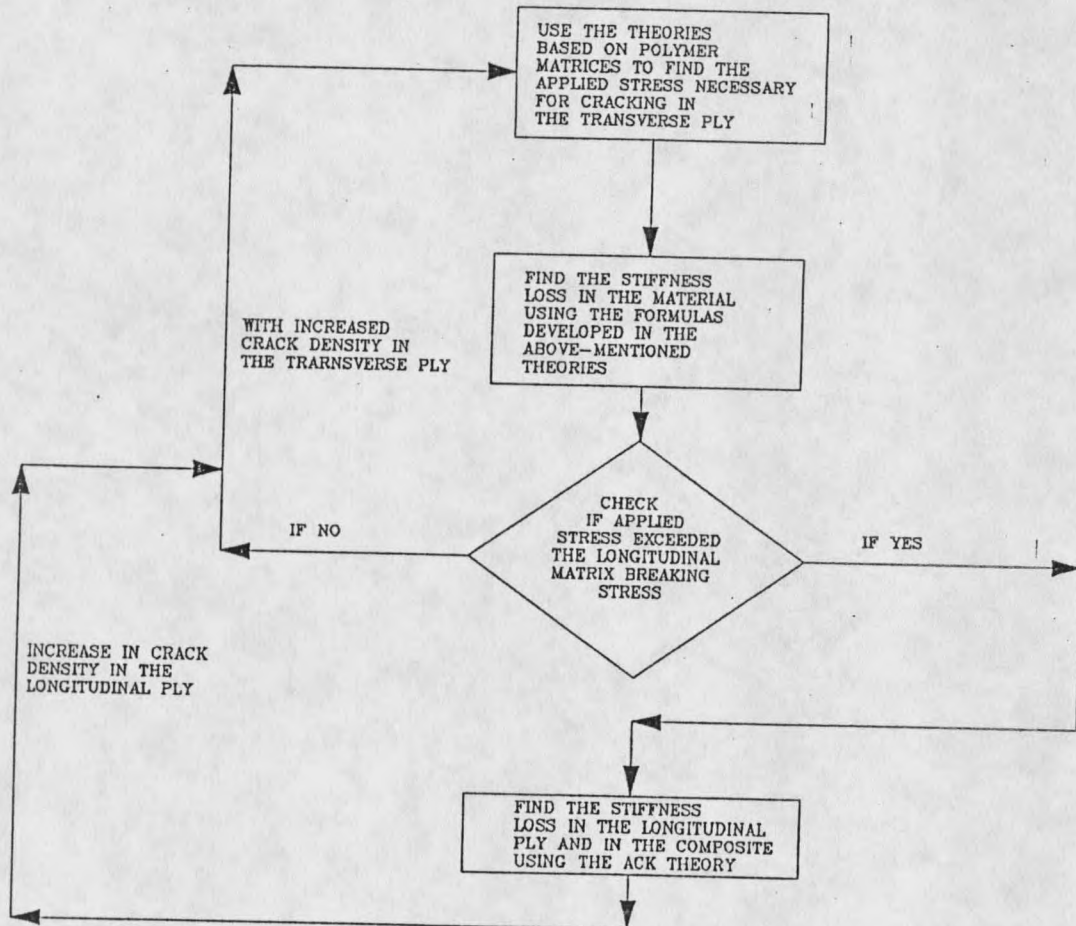
NICALON/CAS-II

$b=d$	=	0.2 mm
E_l	=	136.62 GPa
E_t	=	117.24 GPa
E_o	=	110.35 GPa
G_{23}	=	45.82 GPa
α_{lm}	=	$4.530 \times 10^{-6} / ^\circ$
σ_{R^m}	=	+15.72 MPa
σ_{R^t}	=	-15.72 MPa
σ_{R^l}	=	0.0162 %
ϵ_{tpf}	=	0.055 % (exptl)
σ_a	=	40.00 MPa (exptl)
G_c	=	41 J/m ²

NICALON/LAS-II

$b=d$	=	0.2 mm
E_l	=	126.0 GPa
E_t	=	82.99 GPa
E_o	=	104.69 GPa
G_{23}	=	45.82 GPa
α_{lm}	=	$2.950 \times 10^{-6} / ^\circ$
σ_{R^m}	=	-4.07 MPa
σ_{R^t}	=	+4.07 MPa
σ_{R^l}	=	-0.0057 %
ϵ_{tpf}	=	0.094 % (exptl)
σ_a	=	71.00 MPa (exptl)
G_c	=	37 J/m ²

Appendix B

Fig. 31 Computer Flow Diagram

Appendix C

Fig.32 Computer Code for Modified Laws-Dvorak Theory

```

c this program is written to calculate the stiffness loss
c in a cross-ply composite undergoing cracking. The
c progressive cracking is assumed to take place at the mid-
c point of the ply. The applied stress to cause additional
c cracking is also calculated. This is based on the Norman
c Laws and Dvorak theory.
c
c ***** DOCUMENTATION *****
c
c      b      = thickness of the outer 0(longitudinal) ply
c      2d     = thickness of the inner 90(transverse) ply
c      Et     = youngs modulus of the transverse ply
c      El     = youngs modulus of the longitudinal ply
c      Ec     = youngs modulus of the composite
c      slr    = residual stress in the longitudinal ply
c      srt    = residual stress in the transverse ply
c      sigma  = applied stress needed to cause cracking
c      Em     = matrix modulua
c      Ef     = fiber modulus
c      r      = radius of the fibers
c      tau    = fiber-matrix interface bond strength
c      emu    = matrix failure strain
c *****
c
c VARIABLES
c      PARAMETER (ly=40)
c      IMPLICIT REAL*8 (a-h,o-z)
c      DIMENSION Sigma(ly)
c Open input and output files
c      OPEN(UNIT=11,FILE='1723.IN',STATUS='OLD')
c      OPEN(UNIT=12,FILE='stls.mat',STATUS='UNKNOWN',
c + FORM='FORMATTED')
c      OPEN(UNIT=13,FILE='nic.MAT',STATUS='UNKNOWN',
c + FORM='FORMATTED')
c      OPEN(UNIT=14,FILE='nic1.MAT',STATUS='UNKNOWN',
c + FORM='FORMATTED')
c Read in the variables
c      READ(11,*) b,d,Et,El,Ec,Em,Ef,Vm,Vf,Gc,srt,emu,r,tau
c
c      read(*,*)sfpf1
c      read(*,*)pq
c      slr=-srt
c      El2=El
c      i=1
c      sfpf=22.64
c Calculate the shear lag parameter
c      sai= d*(b+d)*Et/(b*El*Ec*Gc)*(sfpf1+(Ec*srt/Et)**2

```

```

write(*,*)sai
alpha= (Em*Vm)/(Ef*Vf)
x1 = (Vm/Vf)*Em*emu*r/(2*tau)
c Calculate the value of crack density parameter
READ(11,*) b1,b2,nb
db=(b2-b1)/nb
bt=b1+db
bt1=b1+db
c Find out the applied stress for the various values of
c crack density and check for longitudinal ply matrix
c cracking. If the matrix cracking initiates in the
c longitudinal ply, put the residual stress as zero.
DO 10 k=1,nb
+ Sigma(k)=(sfpf+Ec/Et*srt)*1/(dsqrt(2*
dtanh(sai/(2*bt))-dtanh(sai/bt)))-Ec/Et*srt

Eb=Ec/(1+(bt*d*Et*dtanh(sai/bt))/sai/b/E1)
Eboc=1/(1+(bt*d*Et*dtanh(sai/bt))/sai/b/E12)

if (Sigma(k).lt.100) then
write(*,*)'long. failure stress hasnt reached'
else
bt2=bt1/b/2
temp=(1+alpha/2)
E12=E1/(temp*(2*bt2*x1+(1-2*bt2*x1)/temp))
per=(E1-E12)/E1*100
Ec=Ec-Ec*per/100
E1=E12
srt=0
if (i.eq.1) then
temp1=(sfpf1+(Ec*srt/Et))**2
sai= d*(b+d)*Et/(b*E1*Ec*Gc)*temp1
i = 2
else
continue
endif
bt1=bt1+pq
end if
c Calculate the crack density
cd=bt/d/2
WRITE(12,*)Eboc
WRITE(13,*)Sigma(k)
WRITE(14,*)cd
10 bt=bt+db
write(*,*)sai
c
END

```

Appendix D

Fig.33 Computer Code for the Modified Nairn's Theory

```

c This program is written to calculate the stiffness loss
c in a cross-plyed composite undergoing cracking. The
c progressive cracking is assumed to take place at the mid-
c points of the existing cracks. The applied stress to
c cause additional cracking is also calculated. This is for
c nicalon/1723. This uses modified Nairn's analysis.
c
c ***** DOCUMENTATION *****
c
c      b      = thickness of the outer 0(longitudinal) ply
c      2d     = thickness of the inner 90(transverse) ply
c      Et     = youngs modulus of the transverse ply
c      E1     = youngs modulus of the longitudinal ply
c      Ec     = youngs modulus of the composite
c      ert90  = thermal residual strain in the transverse
c              ply
c      G23    = shear modulus
c      srt    = residual stress in the transverse ply
c      sfpf90 = first ply failure stress
c
c *****
c
c Variables
c   PARAMETER (ly=200)
c   IMPLICIT REAL*8 (a-h,o-z)
c   integer cd
c   DIMENSION LOAD(ly)
c   COMMON/TEST/alpha,beta,flag
c Open input and output files
c   OPEN(UNIT=11,FILE='17231.IN',STATUS='OLD')
c   OPEN(UNIT=12,FILE='stls.mat',STATUS='UNKNOWN',
c + FORM='FORMATTED')
c   OPEN(UNIT=13,FILE='nairn1.MAT',STATUS='UNKNOWN',
c + FORM='FORMATTED')
c   OPEN(UNIT=14,FILE='nairn2.MAT',STATUS='UNKNOWN',
c + FORM='FORMATTED')
c Read in the variables
c   READ(11,*)d,Et,E1,Ec,ert90,G23,srt,Eco,sfpf,Em,Ef,Vm,
c       Vf,alphaT,alphaA,T,vT,vA,GT,Gc
c
c   GA=GT
c   delalpha=alphaT-alphaA
c   lambda=b/d
c   h=2.*(b+d)
c   C1= h*Ec/(b*E1*Et)
c   C2= vT/Et*(lambda+2/3)-vA/E1*lambda/3.

```

```

C3= (lambda+1)/(60*Et)*(3*lambda**2+12*lambda+8)
C4= 1./3.*(1/GT+lambda/GA)
q=C1/C3
p=(C2-C4)/C3
flag=4*q/(p**2)
call val(flag,p,q,alpha,beta)
i=1
c begin the loop for calculating the applied stress for
c various crack densities
do 10 cd = 100,5000,50
rho1 = 1/(2.d0*cd)
rho = 2.* rho1/d
t1 = (delalpha*T/C1)**2
func1=(Gc/(d*C3*(2.*Xchi(rho/2.0)-Xchi(rho)))-t1)
LOAD(i)= Ec/Et*sqrt(func1)
write(13,*)LOAD(i)/1000000.
write(14,*)cd/1000.
10 i=i+1
c END OF THE MAIN PROGRAM
end

```

```

real*8 function xchi(chi)
c variables
real*8 p1,p2,p3,p4,chi,alpha,beta,flag
common/test/alpha,beta,flag
c begin function
if (flag.gt.1) then
p1=(dcosh(2.d0*alpha*chi)-dcos(2.d0*beta*chi))
temp=beta*dsinh(2.*alpha*chi)
temp1=alpha*dsin(2.*beta*chi)
p2=temp+temp1
Xchi=2.*alpha*beta*(alpha**2+beta**2)*p1/p2
else
temp3=(beta**2-alpha**2)
p3=temp3*dtanh(alpha*chi)*dtanh(beta*chi)
p4=(beta*dtanh(beta*chi)-alpha*dtanh(alpha*chi))
Xchi=alpha*beta*p3/p4
endif
return
end

```

```

SUBROUTINE VAL(flag,p,q,alpha,beta)

```

```

c parameters
real*8 flag,p,q,alpha,beta
if (flag.gt.1) then
theta=atan(sqrt(4*q/(p**2)-1))
alpha=q**.25*cos(theta/2)
beta=q**.25*sin(theta/2)
else
alpha=sqrt(-p/2+sqrt(p*p/4-q))
beta=sqrt(-p/2-sqrt(p*p/4-q))

```

MONTANA STATE UNIVERSITY LIBRARIES



3 1762 10072483 8

